DOE/NASA/1040-80/11
NASA TM-81433

FUEL ECONOMY SCREENING STUDY OF ADVANCED AUTOMOTIVE GAS TURBINE ENGINES

John L. Klann
National Aeronautics and Space Administration
Lewis Research Center

March 1980

Prepared for
U.S. DEPARTMENT OF ENERGY
Conservation and Solar Applications
Transportation Energy Conservation Division

NOTICE

DOE/NASA/1040-80/11
NASA TM-81433

FUEL ECONOMY SCREENING STUDY OF ADVANCED AUTOMOTIVE GAS TURBINE ENGINES

John L. Klann
National Aeronautics and Space Administration
Lewis Research Center
Cleveland, Ohio 44135

March 1980

Work performed for
U. S. DEPARTMENT OF ENERGY
Conservation and Solar Applications
Transportation Energy Conservation Division
Washington, D. C. 20545
Under Interagency Agreement EC-77-A-31-1040

FUEL ECONOMY SCREENING STUDY OF ADVANCED AUTOMOTIVE GAS TURBINE ENGINES

by: John L. Klann
Lewis Research Center

SUMMARY

An analytical study was made to compare potential fuel economies among ten turbomachinery configurations for advanced, high-temperature, gas-turbine engines. During this configuration screening a common set of design parameter values was assigned for the advanced gas-turbines. The best fuel economy over the composite driving cycle was calculated for each of the ten engines mated to a continuously variable speed-ratio transmission in a 1978 compact car. A reference value of fuel economy was calculated for the car with its conventional spark-ignition piston engine and automatic three-speed transmission. The best advanced free-turbine engine was also evaluated with this conventional transmission. The sensitivity of fuel economy to changes in engine design parameter values was evaluated for both the best free-turbine engine with the conventional transmission, and the best fixed-geometry single-shaft engine with the variable transmission. All calculations assumed gasoline as the fuel and a 29°C (85°F) day. A design turbine-inlet temperature of 1370°C (2500°F) and ceramic turbine rotors were assumed.

The best fuel economy among fixed-geometry configurations was a 55% gain over the reference value for the spark-ignition piston engine. This configuration was a single-shaft engine that had a single-stage radial turbine with its tip speed limited to 610 m/s (2000 ft/sec). A 60% gain over the reference fuel economy was calculated for the combination of the best free-turbine configuration and the conventional transmission. The gas-generator shaft of this configuration had a single-stage radial turbine and the output shaft had a single-stage axial turbine with variable nozzles.

The best fuel economy among variable-geometry configurations was a 67% gain over the reference value. This configuration added both variable turbine nozzles and variable compressor-diffuser vanes to the best single-shaft fixed-geometry configuration. Free-turbines with this degree of variable geometry were not included in the study. No advantage in fuel economy was found for a two-stage turbine over a single-stage turbine among the single-shaft configurations. For either free-turbine or single-shaft configurations, there was a fuel economy advantage for a radial-turbine stage over an axial-turbine stage. Sensitivity results showed a further gain of 4 to 5% in fuel economy if a single-stage radial-turbine tip speed of about 740 m/s (2400 ft/sec) were practical. With tip speeds limited to 610 m/s (2000 ft/sec) and a design turbine-inlet temperature of 1370°C (2500°F), an engine with a regenerator capability of about 1040°C (1900°F) was sufficient for near-peak fuel economy.

E-357

The free-turbine/conventional transmission combination showed less sensitivity to fuel economy with engine design power output than did the single-shaft engine/variable transmission combination. However, more detailed analysis would be required to quantify any relative differences. No first-order differences in sensitivity were calculated due to changes in design performance level for the single-shaft engine.

INTRODUCTION

Advanced gas-turbine engines for automobiles are being developed under a cooperative government-industry effort. This development program is sponsored by DOE with project responsibilities delegated to NASA-Lewis Resarch Center. The study reported here was made to provide general background information for the program. Fuel economies were calculated over the EPA (Environmental Protection Agency) composite driving cycle and are presented for relative comparisons among ten advanced gas-turbine engine configurations and to a conventional spark-ignition engine in the same car. Because of simplifying assumptions and uncertainties in technology projections, the absolute fuel economies calculated for the gas-turbine engines are not necessarily those which may be attained as a result of the program. However, the results do provide a relative evaluation, or screening, among the advanced gas-turbine engine configurations. A design turbine-inlet temperature of 1370°C (2500°F)(1) and ceramic turbine rotors with a tip-speed limit of 610 m/s (2000 ft/sec) were assumed.

Earlier government study results on this subject are presented in references 1 and 2. And, results of four government-funded studies of Improved Automotive Gas-Turbine Powertrains are presented in references 3 through 6. These independent contractor studies also examined choices among potential engine configurations. Two (ref. 3 and 5) preferred a single-shaft engine, while the other two preferred a free-turbine engine. The results presented here were generated at the same time as the results from these contractor studies. With them, the reader may gain some added perspective for fuel-economy trade-offs since some engine/transmission combinations evaluated here were not considered by the contractors.

Six single-shaft and four free-turbine engines were studied here. Variations among the engines allowed an evaluation of the effects of variable turbomachinery geometry, of one- and two-stage turbines, and of radial against axial turbine stages. Best fuel economy was determined for each engine configuration using common design parameter values, characteristics of a 1978 compact car, and a generalized model for a continuously variable speed-ratio transmission. A reference fuel economy was calculated for the car with its conventional spark-ignition piston engine and three-speed automatic transmission. One free-turbine engine was also analyzed with the three-speed automatic transmission and with a specific model for a traction-type continuously variable transmission from reference 3.

Two of the more promising engine and transmission combinations were also studied for sensitivities to fuel economy. Sensitivities were determined by changing each major gas-turbine design parameter value, one at a time from the base set, re-designing each engine and

(1) English units were the base units in this study.

re-optimizing for best fuel economy. One of the two promising combinations was also studied about a revised set of design values to evaluate the effects of a lower-level of gas-turbine performance on the calculated sensitivities.

Calculated and measured results for the reference spark-ignition piston engine are presented first, followed by a comparison of results between variable transmission models. Fuel economy comparisons are then made among the gas-turbine engines and transmission combinations. The sensitivity results are presented last.

ENGINE CONFIGURATIONS

The reference spark-ignition piston engine used in this study had six cylinders with 3800 cm^3 (232 in^3) displacement. It produced a maximum net output to the transmission and vehicle accessories of 69 kW (92 hp) at 3600 rpm.

The ten gas-turbine configurations studied here are listed in table I. The variations among the configurations involved the turbomachinery. All configurations used a single-stage, radial compressor and an engine-driven rotary regenerator. A speed-reduction gear box for input to the transmission was assumed to be a part of the configurations. One single-shaft configuration used a single-stage, radial turbine, others used two-stage turbines; the first stage of which was either radial or axial. The free-turbine configurations used either a single-stage radial or axial turbine on the gas-generator shaft, and only a single-stage axial turbine on the free-turbine shaft.

Three variable geometry features were studied among the single-shaft configurations. Configuration number two added variable compressor-inlet guide vanes to configuration one. Configuration three added variable turbine nozzles to configuration one. Configuration number four added variable compressor-outlet guide (diffuser) vanes to configuration three. The free-turbine configurations considered only variable free-turbine nozzles. As noted in table I, configuration acronyms are defined in Appendix A.

METHODS OF ANALYSIS

Two separate computer codes were used. One was for gas-turbine design and off-design performance. The other was for analyzing vehicle fuel economies. Gas-turbine calculation methods and assumptions are presented first, followed by those for determining fuel economy. Then, the assumed car and transmission characteristics are presented. Details of the methods used for determining fuel-economy sensitivities are presented last.

Gas Turbines

Design and off-design performance of each gas-turbine configuration was analyzed with the use of a modified version of the Navy/NASA Engine Program (NNEP, ref. 7). This versatile code was originally developed for the analysis of aircraft gas-turbines. Engine configurations are described by input to NNEP. A design-point calculation occurs first, followed by off-design calculations. Off-design component performance is input to the code in tables as functions of up to three variables. Hence, NNEP can accomodate turbomachinery maps with variable geometry. Other features of NNEP include optimization subroutines and the ability to limit any desired engine variable. Variable-geometry turbomachinery settings were optimized with NNEP to produce least fuel consumption at each off-design engine operating condition. Limit variables were used to control turbine-inlet temperature whenever regenerator-inlet temperature reached a prescribed maximum value.

For each configuration, design compressor pressure ratio was treated as an independent variable. Hence, each configuration was examined over a range of design pressure ratios. NNEP predicted values of engine power and fuel consumption as functions of percent engine output speed. These values were used as input to the driving-cycle code. Comparison of resulting fuel economies from the driving-cycle code permitted a selection of the best design compressor pressure ratio for each configuration.

NNEP Modifications. Since NNEP was originally developed as an aircraft engine program, several modifications and additions were needed for the purposes here. The modifications included: changing the scaling method for heat-exchanger effectiveness from one linear with E* (symbols are defined in Appendix B) to one based on $E^*/(1-E^*)$; and, re-defining heat-transfer effectiveness from a cold- and hot-inlet specific heat basis to one based on actual enthalpy change. The additions to NNEP included subroutines for computing preliminary design estimates of size, velocity diagram, and efficiency of each turbomachinery component; and outputting engine performance in forms suitable for direct input to the driving-cycle code.

Design Characteristics and Assumptions. The base set of gas-turbine engine and component parameter values assigned for the configuration screening are presented in table II. The assigned values are generally optimistic but, in general, potentially achievable. Calculation procedures and associated assumptions are discussed below by categories.

1. Engine Power Outputs. Assigned values are presented in table II(A). Engine net power output is defined as that available to the transmission and vehicle accessories. Gross engine power output includes the power required to operate engine accessories; namely, the regenerator drive and the fuel pump. Design net power was set at a level that was representative of that needed to give a reasonable acceleration time for the weight-class car assumed here. Idle net

power was set based on the needs of the vehicle accessories and the torque converter that was a part of the automatic three-speed transmission. The assigned idle power resulted in an engine idle speed of 600 rpm. The same idle power was assumed with the continuously variable transmission. Both design and off-design engine performance was calculated for SAE (Society of Automotive Engineers) standard test conditions with gasoline as the fuel.

2. Pressure Losses. Assigned design values for pressure loss ratio, $\Delta P'/P'$, are presented in table IIB by engine component. The sum of all the pressure loss ratios is .135 for a single-shaft configuration, and .160 for a free-turbine configuration. The two-stage turbines in the single-shaft configurations were assumed to be closely coupled with no pressure drop between stages. However, the two turbine stages in the free-turbine configurations were separated and used an interstage duct with an added pressure drop. Off-design variations in all component pressure drops were assumed to be only functions of relative inlet corrected mass-flow rate to each component. These normalized variations are shown in figure 1. Regenerator data were from reference 8, the other data were from reference 9. Absolute pressure drop, $\Delta P'$, increases with increasing flow for each duct or heat exchanger component, and most pressure loss ratios also increase with increasing flow. However, the reverse trend in pressure loss ratio occurs for the cold side of the regenerator because there the inlet pressure increases faster than the absolute pressure drop.

3. Compressor Efficiency and Performance. The subroutines added to NNEP for turbomachinery design estimates made both compressor and turbine efficiency dependent variables in the analysis. Compressor efficiency was based on the total-to-total pressure ratio from the impeller inlet to the diffuser exit. Table II(B) shows the further design pressure drop that was assumed for the compressor-outlet scroll. Basic correlations for radial-compressor peak efficiencies are shown in figure 2. Compressor efficiency was a function of design pressure ratio, specific speed, and equivalent mass-flow rate. These efficiencies are somewhat higher than those used in reference 1. They are the result of analytically optimizing compressor geometry with the use of an updated version of the computer code described in reference 10. The optimizations were made assuming impeller splitters, a diffuser leading-edge Mach number of 0.9, and a diffuser-exit Mach number of 0.13. The peak efficiencies determined from the compressor computer code are based on detailed loss correlations, which are felt to be obtainable within the future capabilities of three-dimensional design analysis and experimental development.

The peak efficiencies from figure 2 were subject to two decrements before being assigned as the design-point values for any compressor. These decrements, table II(B), were for the presence of variable geometry, or for performance-map corrections. The variable-geometry decrements were based on judgement, but were felt to be representative of the added losses that would be incurred. The performance-map

decrements accounted for differences between peak- and design-point efficiencies on the particular compressor performance maps that were used in NNEP with any particular engine configuration. Table III(A) shows that three sets of compressor performance maps were used. Table III(B) indicates the configuration usage. Both experimental and analytical performance maps were used. The analytical compressor performance maps were obtained from a modified version of the code described in reference 12. Performance-map efficiency decrements are given in table III(A), and the sum of all design efficiency decrements is given by configuration in table IV.

Compressor performance from NNEP was a function of the calculated and corrected efficiency at the design point, and the particular set of peformance maps used for that configuration. The design-point values on each of the three sets of performance maps were specified similarly at 100 percent corrected speed, slightly below choked corrected mass-flow rate. The map design-point values were set equal to the calculated design-point conditions being investigated. The rest of that performance map was normalized and scaled by generating linear factors (ref. 7) for efficiency, pressure ratio, and corrected mass-flow rate and speed.

4. Regenerator Performance. A base design value for effectiveness of 0.94 was assigned. Packaging studies of reference 5 show that the required volume of such a regenerator can fit in a compact car. Off-design effectiveness, shown in figure 3, was a function of cold-side mass-flow rate. These are scaled results from the data of reference 8.

Regenerator seal leakage flow rates are shown in figure 4 and are expressed as a percent of the engine-inlet mass-flow rate against design compressor pressure ratio. The curve labelled "base values" was used for the screening part of the analysis. Off-design seal leakage flow rates were assumed to be a constant percentage of the engine-inlet mass-flow rate.

Table II(B) also indicates the assumed seal leakage distribution. The flow across the cold face is from the high-pressure inlet to the low-pressure outlet. Carryover flow is from the high-pressure inlet to the low-pressure inlet. And, the flow across the hot face is from the high-pressure outlet to the low-pressure inlet.

5. Combustion and Engine Heat Losses. No particular type of combustor was specified and typical gas-turbine performance parameters were assumed (table II(B)). The value for combustor efficiency was assumed to be constant for all engine calculations. No engine heat losses were assumed.

6. Turbine Efficiency and Performance. All turbine efficiencies were analyzed as total-to-total values from stator inlet to rotor outlet. The first turbine in an engine configuration was assigned an

additional total-pressure drop for an inlet scroll or a transition duct from the combustor. The last turbine in an arrangement was assigned a diffuser total-pressure loss.

Basic correlations for peak radial-turbine efficiency are shown in figure 5. Turbine efficiency was a function of specific speed, equivalent mass-flow rate, and blade-to-jet speed ratio. Figure 5a shows the efficiencies for best values of design blade-to-jet speed ratio. Figure 5b shows the efficiency correction factor when radial-turbine tip speed was limited. These are the same efficiency correlations as those used in reference 1, but without the diffuser-exit loss or the .02 degradation in efficiency that was allowed for ceramic fabrication. The assumption here was that with future improvements in design analysis techniques, and with experimental development, the same levels that are now achieved with metal rotors can also be obtained with ceramic rotors.

Typical variations for peak axial-turbine efficiency are presented in figure 6. Axial-turbine efficiency was a funtion of speed-work parameter and Reynolds number. The Reynolds number range in figure 6 was typical for this application. The correlations were from the analysis of reference 13 with the use of symmetrical velocity diagrams. No efficiency degradation was assumed for ceramic rotors.

As in the case of the compressor, the peak efficiencies for both types of turbines were subject to the same two types of decrements, table II(B), before being assigned as the design-point values. The variable-nozzle loss for radial turbines was assumed to be less than that for axial turbines because of the parallel nozzle walls, and therefore easier clearance control than with the annular nozzle walls with axial turbines.

Design efficiency decrements due to the turbine performance maps used in the analysis are presented in table III(A). Three sets of performance maps were used for radial turbines, and three others for axial turbines. The radial-turbine maps were obtained from the computer code described in reference 14. The analytical axial-turbine maps were obtained from the code described in reference 15. The design-point values on each turbine performance map were specified similarly at 100 percent corrected speed and at a corrected mass-flow rate just less than that at choking. The map normalizations and scaling procedures in NNEP were the same as for the compressor.

7. Operational Engine Temperatures. All hot-section components including turbine rotors were assumed to be ceramic. Therefore, a design turbine-inlet temperature (table II(B)) of 1370°C (2500°F) was assumed to be a practical goal. This temperature was also the highest operating temperature. During off-design operation, turbine-inlet temperature was controlled such that the hot-side regenerator-inlet temperature did not exceed 1038°C (1900°F). Thus, during off-design engine operation, turbine-inlet temperature was maintained at 1370°C

(2500°F) until the hot-side regenerator-inlet temperature of 1038°C (1900°F) was reached. Then, turbine-inlet temperature was reduced such that the regenerator limit of 1038°C was maintained until idle speed was reached. At idle speed, all temperatures were decreased to reduce power output to 1.9 kW (2.5 hp). This operational limit was assumed for the advanced ceramic engines. Current experimental ceramic regenerators (ref. 8) have successfully operated at hot-inlet temperatures of 1000°C (1832°F).

8. Maximum Turbine-Tip Speed. Internal studies at Lewis indicate that tip-speeds in the range of about 600 to 670 m/s (2000 to 2200 ft/sec) may be within the level of technology for ceramic materials in the 1990s. A maximum (design) turbine-tip speed limit of 610 m/s (2000 ft/sec), table II(B), was used for the screening part of this study.

9. Turbomachinery Shaft Parameters. Single-shaft and gas-generator design shaft speed was set at 100,000 rpm, table II(B). This value was chosen, based on a preliminary design analysis with NNEP, to give high design values of turbomachinery efficiency for this application. A 50% idle speed was used for both single-shaft engines and the gas-generator shaft of free-turbine engines, independent of any variable geometry. Design shaft speed for free-turbines was calculated by specifying the design parameter values shown in table II(B).

A total value for all parasitic shaft losses was assigned for each shaft arrangement at the design point. These would include the engine accessory loads, and bearing, seal, disk windage, and output speed-reduction gear losses. The assumed values in Table II(B) are lower than most current designs and may be difficult to obtain even with advanced technology. The normalized off-design variation for shaft parasitic loads is shown in figure 7 and was obtained from reference 9.

Design values for turbomachinery shaft-seal leakage mass-flow rates are presented in figure 4. These values are typical of current technology and no further reduction in these losses was assumed. Off-design flow rates were a constant percent of the engine-inlet mass-flow rate. All of this leakage flow was distributed to the turbine-rotor inlets and was assumed to be at compressor-outlet temperature when mixed with the turbine flow.

Fuel Economies

Input to the driving-cycle code from NNEP was different depending on the type of transmission being used. With a continuously variable transmission, the input consisted of single variations of engine net output power and minimum fuel-flow rate as functions of percent engine output speed. With the automatic three-speed transmission, the required input was a matrix of engine net output power and fuel-flow

rate as functions of percent engine output speed.

The separate computer code for calculating fuel economies over the composite driving cycle is undocumented. Composite fuel economy is a harmonic average of fuel economies for both city and highway driving cycles as specified in Federal Test Procedures. Vehicle speed for each second of the cycles is specified in the Federal Register. The computer code used the average vehicle speed during each one-second interval in both cycles.

The city-cycle test procedure includes both a cold- and hot-engine start-up. A portion of the extra fuel required for the cold start is added to the total fuel that is consumed during the cycle with a hot start. This is called the warm-up penalty for the city driving cycle. In this analysis, however, no attempt was made to compute warm-up fuel penalties for gas-turbine engines. Hence, the absolute fuel economies reported here for gas-turbine engines do not include warm-up penalties.

Reference 5 indicates that the warm-up fuel penalty for spark-ignition piston engines reduces city-cycle fuel economy by seven percent. This factor was used here to compare calculated versus measured fuel economy for the reference spark-ignition piston engine/car. Relative fuel economies that are presented for gas-turbine engines with respect to the reference spark-ignition engine were computed neglecting warm-up fuel for both engines.

Calculation procedures in the driving-cycle code started at the vehicle wheels. The power required at the wheels of the car was specified by the sum of the steady-state (road-load) power to overcome drag and rolling resistance at a constant car speed; the power needed to accelerate the car; and the power needed to accelerate the wheels themselves. Powertrain speeds were specified by assigned values for tire size and various powertrain gear ratios. Powertrain losses were a function of the type of transmission, various powertrain speeds, and the level of power being transmitted. All powertrain and engine inertias other than the wheels were assumed to be small and their effects on power needs were neglected. Vehicle accessory power needs were a function of transmission-input speed. Required engine power was determined by the sum of the power required at the wheels, the powertrain losses, and the vehicle accessory needs at each second in the driving cycles. With a continuously variable transmission, engine speed was set at the value which gave least fuel consumption. With the automatic three-speed transmission, engine speed was a function of the current gear ratio. Shift logic among transmission gears was a function of power level, car speed, and whether the car was accelerating or decelerating.

Car and Transmission Characteristics

Parameter values assigned for all fuel economy calculations are listed

in table V. The only gasoline property needed was that of density. The lower heating value (table II(A)) for gasoline was used in NNEP to determine engine specific fuel consumption.

A 1978 compact car was assumed with the test weight shown in table V. Curb weight would be 136 kg (300 lbm) lighter. The car's road-load power needs are shown in figure 8 and were obtained from reference 6. The assumed vehicle accessory loads are shown in figure 9. They consist of a power-steering pump load and an alternator power need. These were used independent of transmission type. The alternator load in figure 9 is typical of a small amount of engine electric control power and the load due to windage.

The drive-axle gear ratio and wheel parameter values in table V are also representative of the assumed compact car. The drive-axle efficiency was approximated as a constant. Reference 16 makes a similar assumption at a lower efficiency level and indicates a small error in this approach at light loadings.

The generalized model for the efficiency of a continuously variable speed-ratio transmission is shown in figure 10. Transmission efficiency was a function of car speed and also, above 16 kph (10 mph) a function of percent engine output power. The variation with power was assumed to be linear. All transmission losses, such as pump, bearing, and mesh losses, are included in this transmission efficiency. This model was based on an approximation of efficiency results found in the literature for both traction and hydromechanical types of continuously variable transmissions when used with gas-turbine engines.

One cross-check was made and is presented between the model in figure 10 and that of reference 3 for a traction-type continuously variable transmission. In the model of reference 3, transmission efficiency was analyzed from its constituents. A two-speed range gear set was used, each with a traction efficiency of 85 percent. Mechanical efficiency was determined then as a function of the percent of maximum speed ratio between the engine and output shaft. Inclusion of bearing and mesh losses resulted in overall transmission efficiency. In contrast to the model in figure 10, the efficiency for the model of reference 3 was dependent on required transmission speed ratio.

The performance of the automatic three-speed transmission was analyzed as a combination of a front pump, a torque converter, and a gearbox. The transmission pump power needs are shown in figure 9. Torque converter performance curves are presented in figure 11, while gearbox efficiencies are presented in figure 12; these were obtained from reference 6.

Average transmission efficiencies over the driving cycles are presented in the results. These were calculated only over those time portions of the driving cycles when power was being supplied to the

wheels of the car. The value for the composite cycle was defined as the harmonic average of those for the city and highway cycle.

Sensitivities

The general approach to the sensitivity part of this analysis was to study the effects on composite fuel economy of changes in the assigned values for each major engine and component parameter from the base set (table II), one at a time. Each parameter-value change caused a new engine design which was re-optimized for design compressor pressure ratio. Hence, the calculated sensitivities for fuel economy reflect changes in both design and off-design engine operation, and are not the sensitivities of changes to a fixed-engine design. The only parameter values in table II not studied for sensitivity effects were the fuel characteristics and ambient engine conditions. It should be noted, however, that component pressure loss ratios were not studied individually, but were varied together.

Since performance sensitivities can be dependent on the general level of engine performance, additional sensitivity calculations were made around a second, or more conservative, set of engine and component parameter values. Table VI lists those values which were assumed to be different between the conservative set and the base set and were used in the study of single-shaft engine sensitivities. The turbine and compressor efficiency decrements in table VI are in addition to those in table IV. The lower combustor efficiency in the conservative set (table VI) was used to simulate an engine heat loss equivalent to the energy content of two percent of the fuel.

Figures presented in the Results and Discussion section show plots of the sensitivity results for the parameter changes that were studied. Those plots were used to determine small-change sensitivities which were then used to order the parameters according to importance.

RESULTS AND DISCUSSION

The absolute values for fuel economies presented here are not necessarily those which might be attained in future gas-turbine powered cars. These fuel economies are known to be optimistic because gas-turbine heat losses and warm-up fuel needs were neglected. They are also probably optimistic because not all of the technology advances assumed here are likely to be achieved in a single practical engine. In contrast, the fuel economies are also known to be conservative because no credit was taken for the ability to burn fuels with higher energy content, such as diesel fuel, nor for future vehicle or transmission improvements. The fuel economies of the advanced gas turbine engines relative to the spark-ignition piston engine are also somewhat uncertain for many of the same reasons. Therefore, the reader's attention should be principally directed to relative changes in fuel economy among the gas turbine configurations.

Reference Fuel Economy

Calculated and measured fuel economies are compared in table VII. The measured fuel economies were for the compact car that was modelled here analytically. The analysis did not necessarily duplicate the actual transmission shift logic. However, reasonable agreement between test and calculated fuel economies was expected.

Comparison of columns one and three under Fuel Economies in table VII shows that the calculated composite fuel economy with the estimated warm-up fuel allowance was about two percent lower than the measured value. The calculated highway fuel economy was about four percent low. It does appear, however, that the analysis produced a reasonably close value for composite fuel economy.

The reference value of fuel economy used herein was the calculated composite number, 8.88 km/l (20.9 mpg), without the warm-up fuel penalty. This value was four to five percent higher than either the measured or calculated composite fuel economy with warm-up fuel penalties.

Continuously Variable Transmission Model

Comparison of results between the use of the two models for a continuously variable speed-ratio transmission is made in table VIII. Fuel economies and average transmission efficiencies over the driving cycles are shown. Comparison of composite fuel economies shows that the result of the generalized model was about one percent higher than that of the model of reference 3 for a traction-type transmission. The highway fuel economy with the generalized model was a little lower, while the city fuel economy was somewhat higher. The main reasons for the differences between models are reflected in the computed average transmission efficiencies. The generalized model yielded somewhat higher efficiencies in the city cycle than those of the model of reference 3. However, the reverse was found for the highway cycle such that the average transmission efficiencies for the composite cycle were within .01 of each other. All other results presented here with the variable transmission were obtained with the generalized model.

Gas-Turbine Screening

Results are presented first for the analysis of the fixed- and variable-geometry configurations with the continuously variable transmission. Results are then presented for the best free-turbine configuration using the standard automatic three-speed transmission.

Fixed Geometry. Table IX(A) presents the fuel economy comparisons among fixed-geometry configurations. The single-shaft engine with the single-stage turbine was the only design that was affected by the turbine-tip speed limit. Best design pressure ratios are shown in the

table.

Fuel economies for the single-shaft engines were better than those of the free-turbine engine. The main reason for this was that turbine-inlet temperature could not be maintained for the free-turbines at the same high levels as those of the single-shaft configurations at off-design power outputs. Because of the transmission, the single-shaft engines can be operated at limiting turbine-inlet or -outlet temperatures over the range from idle-to-design engine power. However, with a fixed-geometry free-turbine engine, the only control over gas-generator speed is fuel-flow rate and hence turbine-inlet temperature. The free-turbine engines require reduced turbine-inlet temperature to reduce power output. A comparison of turbine operating temperatures is shown in figure 13. The free-turbine engines also suffer from the additional transition duct pressure loss between the turbines (assumed to be 2.5% at full power) and the extra shaft parasitic losses (assumed to be an extra .75 kW (1 HP) at full power). The overall effects caused the free-turbine engines to have worse off-design specific fuel consumptions and hence poorer fuel economies than the single-shaft engines.

The fuel economy of all three single-shaft engines (table IX(A)) was approximately the same. There was a slight advantage for the engine with the single-stage radial turbine. Its fuel economy was 55% better than that of the reference spark-ignition piston engine. The difference in fuel economy between the free-turbine engines was about 1 km/l (2 mpg) with the advantage for the configuration with the radial turbine on the gas-generator shaft.

The differences in fuel economy among the single-shaft engines and between the free-turbine engines were because of projected variations in turbine efficiency. At the design-point, the combined turbine efficiency for the two-stage, axial-axial turbine was equal to that of the single-stage turbine (.84). The combined efficiency for the radial-axial, two-stage turbine, .86, was greater than that of the single turbine at the design point. However, the off-design efficiency variations, shown in figure 14 resulted in somewhat poorer combined performance for the two-stage turbines and hence for their configurations. Similar results were found between the turbine efficiencies for the free-turbine engines. In both shaft arrangements, however, there was an advantage for a radial turbine stage over an axial stage.

Variable Geometry. Best fuel economies for each of the variable geometry configurations are presented in table IX(B). All variable geometry settings were optimized to provide least fuel consumption over the engine output range for each configuration. Geometry settings for variable turbine nozzles were also limited such that compressor-surge margin was maintained. The best fuel economy in this part of the study was obtained with the largest degree of variable

geometry. That is the single-shaft engine with both variable compressor diffuser vanes and variable turbine nozzles. Its fuel economy was 67% better than that of the reference spark-ignition engine. The fixed-geometry configuration (table IX(A)) showed a 55% improvement in fuel economy. The separate effect on fuel economy of variable turbine-inlet nozzles was a 64% improvement over that of the reference engine. The addition of variable compressor-inlet guide vanes alone was calculated to have a small positive effect on fuel economy. Variable compressor-outlet diffuser vanes when operated alone only tended to choke the compressor and hence led to poorer engine performance. Comparison of tables XI(A) and (B) shows that the addition of variable turbine nozzles to the single-shaft configuration resulted in a lower optimum design compression pressure ratio.

The addition of variable free-turbine nozzles to both free-turbine configurations improved their fuel economy performance. The variable nozzles acted as a flow control device and allowed turbine-inlet temperatures to be maintained at higher levels with reduced output. However, the single-shaft engine fuel economies were still better than those of the free-turbine engines.

The largest effects of variable geometry on single-shaft engine performance are presented in figure 15. Curves of engine specific fuel consumption are compared for configurations one and four. The ordinate in this figure is normalized to a base value. Each variable-geometry engine was designed for full power at the high-flow settings of the variable-geometry components. When variable turbine nozzles were used, an off-design condition resulted through NNEP optimizations which was a more efficient operating condition for full power output. Hence, the variable geometry curve in figure 15 exhibits a better specific fuel consumption over the entire output range.

Each addition of variable geometry to configuration one caused changes in engine operating conditions for the same output power. Figure 16 shows speed-power relationships between configuration one and four. Transitions from constant turbine-inlet temperature operation to constant turbine-outlet-temperature operation are shown in the figure. Power-speed shifts between configuration two or three and configuration one were similar but smaller than those in figure 16. With these shifts, most values of power output with variable geometry were obtained at shaft speeds greater than those with fixed geometry. A major effect of the power-speed shifts was reflected in idle fuel-flow rates. Idle fuel-flow rate for configuration four was 30% lower than that for configuration one; the comparison between configuration three and one was 20% lower; and that between two and one, 5% lower. The idle power level was reached at higher turbine operating temperatures with the speed shifts. Figure 16 shows that idle power, 2.5%, for configuration four was reached at the limiting turbine-outlet operating temperature, while configuration one required a lower temperature.

Each variable-geometry configuration was examined for other major changes in operating conditions as compared to their fixed-geometry configuration. Except for the speed-power shift there were no major operating changes due to the addition of variable compressor-inlet guide vanes. For the same power output, turbomachinery pressure ratios and efficiencies were maintained about the same due to the speed shift. The addition of variable turbine nozzles to configuration one resulted in relatively higher off-design pressure ratios and slightly higher, about .01, compressor efficiencies for the same power output. This was due to operation closer to compressor surge. The combined additions of configuration four resulted in higher operating temperatures and, the highest relative pressure ratios, but lower compressor efficiencies (by as much as .11) for the same part-power output. The lower compressor efficiencies lessened the positive effects of the guide vanes. The additions of variable turbine nozzles to the free-turbine configurations resulted in much higher operating temperatures, but also in reduced power-turbine efficiencies (by as much as .15). Again, this was a negative effect on performance.

Standard Automatic Transmission. The best of the free-turbine engines from table IX was investigated for its fuel economy with the automatic three-speed transmission. This was configuration number eight.

An initial step was to optimize the speed-reduction gear ratio between the engine and tranmission for this configuration. Changes in this gear ratio shift the required power and speed relationships on the engine performance map. Effects of design torque-converter input speed on fuel economy are shown in figure 17. The required speed-reduction gear ratio for best fuel economy was 42.5. All further results for this gas-turbine engine and transmission used this best gear ratio. In practice, such a high gear ratio might require a two-stage gear set and/or an increase in drive-axle gear ratio. Such trade-offs however were beyond the scope of this study.

Best fuel economies and average transmission efficiencies are presented in table X for the free-turbine engine with both types of transmissions. There was no change in best pressure ratio between types of transmissions. Constituent as well as composite fuel economies were better with the conventional transmission. These results were mainly due to the calculated higher efficiencies for the conventional tranmission.

Comparison of relative composite fuel economies between tables IX and X shows that the 60% improvement for the free-turbine and conventional transmission combination makes it competitive with the single-shaft engines and the variable transmission. Therefore, it appears that the two gas-turbine engine and transmission combinations are both logical choices on the basis of fuel economies. From a mechanical point of view there are two trade-offs between these choices. One is the relatively simple single-shaft engine, with or without variable

compressor-inlet guide vanes, against the free-turbine engine with more components and its needed variable free-turbine nozzles. The other trade-off is the complexity and development of a continuously variable speed-ratio transmission against the existing and well-developed conventional automatic, three-speed transmission.

Sensitivities

The screening results for fuel economy showed attractive potentials for either the single-shaft engine, configuration one, using a continuously variable transmission, or the free-turbine engine, configuration eight, using a conventional automatic transmission. Therefore these two engine and transmission combinations were studied further for their sensitivities to fuel economy. For more completeness, the single-shaft engine was studied with both the base set and conservative set of design parameter values. Figures 18 through 30 present results over the parameter ranges which were studied. And, table XI presents a summary of the sensitivity results reduced to small changes about, or near, the respective base values for each case. Specifically, the sensitivity numbers in table XI show the percent change in fuel economy for a $\pm$1% change in each parameter value. Parameters are listed in descending order of importance based on the sensitivities for case A, the single-shaft engine and variable transmission with the base set of design values. Results for turbine-inlet-temperature sensitivities are placed in parentheses to emphasize that no temperature limit was used.

The sensitivity numbers in table XI have been rounded-off to the nearest one or two significant figures, and therefore show only first-order effects near the respective base values for each case. The figures show some second-order effects near the base values (figure 27, for example) and some different sensitivities among the cases for larger parameter changes.

Comparison of sensitivities between the two sets of design values in table XI, case A and B, shows no differences for most parameters. Also the order of importance with the conservative design values (case B) was the same. Shaft losses, regenerator leakage, and idle power all had greater effects on fuel economy sensitivities with the conservative set only because their size was doubled in the conservative set. Hence, no first-order difference in sensitivity to fuel economy near the base values was found due to engine performance level. Although sensitivities were similar between case A and B, relative fuel economies were not. The conservative set of design values resulted in only about a 10% improvement in fuel economy over the reference engine as compared to about 55% for the base set of advanced design values.

Comparison between the two engines and their transmissions in table XI, case A and C, show the same sensitivities except for turbine efficiencies, engine power output, gas-generator idle speed,

turbine-inlet temperature, and shaft parasitic load. The slightly larger sensitivity to shaft parasitic load was again due to the larger base value used with the free-turbine configuration. Also, since the sensitivities to turbine-stage efficiencies with the free-turbine engine were studied separately, each effect on fuel economy was somewhat smaller than that for the single-stage turbine in the single-shaft engine. Specific reasons for the other differences in sensitivities were not found, but are discussed further under separate headings.

Design Power. Calculated variations among the cases with engine design power output are shown in figure 22. The variations are somewhat non-linear, with smaller ratios of change in fuel economy as design power was decreased. As mentioned earlier no specific reason was found for the lower sensitivity for case C, the free-turbine with its conventional transmission. However, the lower sensitivity for case C may have been because this engine and transmission combination operated over a range of fuel consumption rates near but not on the minimum values, and the effects of changes in design power were minimized in such operation. Other potential reasons for the sensitivity difference were also investigated. A slight shift in the best engine speed-reduction gear ratio was found with changes in design power. However, the effect on fuel economy was negligible. Also predicted turbomachinery size effects between engine types, and efficiency variations over the design power range, were similar.

The results in figure 22 indicate that the relative fuel economy performance between engine and transmission combinations may change with design engine power level. However, transmission size effects were not included in the study and could also influence the results. More detailed analysis would be required to fully quantify relative design power-level effects between engine and transmission combinations.

Turbine-Tip Speed. Effects of the assumed design turbine-tip speed limit on the fuel economy of the single-shaft engine are shown in figure 23. Projected 1990s technology for ceramic rotors is shown as a band. Although the small-change sensitivities in table XI show a linear effect on fuel economy, the larger range in the figure shows non-linear changes.

Best aerodynamic values for the turbine occured at a relative design tip speed of about 1.22 (740 m/s or 2440 ft/sec). Composite fuel economy at the best tip speed was about 4% better than that at the base value for case A, and about 5% better for case B. All tip-speed effects were greater with the lower performance level associated with the conservative set of parameter values (case B). Optimum turbine-tip diameter for case A was about 14 cm (5.6 in) with a projected turbine design-point efficiency of 0.86. For case B, optimum diameter was about 18 cm (7.0 in) with an efficiency of 0.83. At the assumed tip-speed limit, turbine diameter for case A was

reduced by 2.5 cm (1 in) and turbine efficiency was reduced by 0.02. The similar decrements for case B were a diameter reduction of 3.0 cm (1.2 in) and an efficiency drop of 0.03.

Idle Speed. Calculated effects of gas-generator idle speed on fuel economy are shown in figure 24. The variations are non-linear, and a slightly larger sensitivity is shown for case C, the free-turbine engine with the conventional transmission. Again, this result is probably due to engine/transmission operation. Variations in specific fuel consumption with free-turbine output speed become larger as gas-generator speed is reduced. And, the free-turbine engine and conventional transmission operates at various combinations of low-power outputs and speeds as required by the driving cycles. The single-shaft engine and the variable transmission, in contrast, always operates at minimum fuel-flow rates.

The trade-off between fuel economy and car acceleration performance with changes in idle speed was beyond the scope of this study.

Operational Temperatures. Figure 25 shows effects of turbine-inlet temperature on fuel economy. The curves resulted from calculations without the turbine-outlet (regenerator-inlet) temperature limit. The symbols show the respective base values for each case with the assumed temperature limit. Single-shaft engine results, case A and B, are shown for best aerodynamic turbine-tip speeds and those at the assumed limiting tip speed. Free-turbine results were not affected by the tip-speed limit and therefore are only for the best tip speeds.

All sensitivities in figure 25 were non-linear. Least sensitivities were obtained with the single-shaft engine and its operation with a limited turbine-tip speed. Because design rotational speed was held constant for the single-shaft engines, higher temperatures and a nearly constant optimum blade-to-jet speed ratio (ν) required increases in turbine diameter and tip speed for best performance. Hence, the turbine efficiency penalty for limiting turbine-tip speed increased with increasing turbine-inlet temperature. In the free-turbine engine (case C) calculations only the gas-generator speed was held constant. The free-turbine design speed, specified by a speed-work parameter (λ) value of one, was allowed to increase with increasing turbine-inlet temperature. The result was a decrease in free-turbine diameter along with an increase in design free-turbine tip speed with increasing design temperature. At a turbine-inlet temperature of 1510°C (2750°F), the free-turbine tip speed was near but slightly below the assumed limiting value. This difference in calculation procedure probably produced the slightly larger sensitivity for case C over that for either case A or B with optimum tip speeds.

Effects of the assumed regenerator-inlet operating temperature limit (1038°C or 1900°F) on fuel economy can be seen in figure 25 by comparing results at a turbine-inlet temperature of 1370°C (2500°F).

With tip-speeds limited to no more than 610 m/s (2000 ft/sec) about a 2% gain in fuel economy was calculated for the single-shaft engine by removing the regenerator temperature limit; a corresponding 1% gain was calculated for the free-turbine engine. The single-shaft engines with best turbine-tip speeds showed either about a 6.5% gain (case B), or about a 5.5% gain (case A), in fuel economy with no regenerator limit. Hence, with turbine-tip speeds limited to 610 m/s (2000 ft/sec) and a design turbine-inlet temperature of 1370°C (2500°F), an engine with a regenerator capable of about 1040°C (1900°F) operation was sufficient for near-peak fuel economy. However, if higher ceramic turbine-tip speeds are attainable in a single stage, higher-temperature regenerator operation might be desirable.

From the results in figure 25, it is seen that the sensitivity of fuel economy to design turbine-inlet temperature, and therefore, the selection of a design turbine-inlet temperature, is dependent on attainable ceramic engine operational limits.

Seal Leakage Rates. Figure 28 presents some additional results for seal leakage mass-flow rates that are not indicated in summary information of table XI. Fuel economy losses due to all engine seal leakages were evaluated. Those due to turbomachinery seals are added vertically to those due to the regenerator seals in figure 28. These results are academic, but do quantify the size of leakage effects on fuel economy.

SUMMARY OF RESULTS

An analytical study was made to compare potential fuel economies among ten turbomachinery configurations for advanced, high-temperature, gas-turbine engines. During this configuration screening a common set of design parameter values for advanced gas-turbines was assigned. Fuel economy over the composite driving cycle was calculated for all gas-turbine configurations with a continuously variable speed-ratio transmission in a 1978 compact car. The best free-turbine configuration and a spark-ignition piston engine were also evaluated with a conventional three-speed automatic transmission. The sensitivity of fuel economy to changes in the design parameter values were evaluated for both the best free-turbine configuration with the conventional transmission, and the best fixed-geometry single-shaft configuration with a variable transmission. All calculations assumed gasoline as the fuel and a 29°C (85°F) day.

The major results of this study were:

1. The best fuel economy for a free-turbine configuration was calculated with the conventional transmission and showed a 60% gain in fuel economy over that for the reference spark-ignition piston engine. This free-turbine configuration had a single-stage radial turbine on the gas-generator shaft and a single-stage axial turbine with variable nozzles on the output shaft.

2. The best fuel economy among fixed-geometry configurations was a 55% gain over that of the reference spark-ignition piston engine. This configuration was a single-shaft engine that had a single-stage radial turbine with its tip-speed limited to a maximum of 610 m/s (2000 ft/sec).

3. The best fuel economy among variable-geometry configurations was a 67% gain over that of the reference spark-ignition piston engine. This gain was obtained by adding both variable turbine nozzles and variable compressor-diffuser vanes to the best fixed-geometry configuration. Free-turbine engines were not studied with this degree of variable geometry.

4. Differences in fuel economy due to the number and type of turbine stages were not large. No advantage was found for a two-stage turbine over a single-stage turbine among the single-shaft configurations. For either free-turbine or single-shaft configurations there was an advantage for a radial-turbine stage over an axial-turbine stage.

5. Sensitivity results showed that a further gain of 4 to 5% in fuel economy might be obtained if a single-stage radial turbine-tip speed of about 740 m/s (2400 ft/sec) were practical.

6. With turbine-tip speeds limited to 610 m/s (2000 ft/sec) and a design turbine-inlet temperature of 1370°C (2500°F) an engine with a regenerator capable of operation up to about 1040°C (1900°F) was sufficient for near-peak fuel economy.

7. Differences in sensitivity to fuel economy between engine and transmission combinations were found for changes in design output power, turbine-inlet tmperature, and gas-generator idle speed. The free-turbine engine/conventional transmission combination showed less sensitivity to design power and slightly greater sensitivity to turbine-inlet temperature and idle speed than did the single-shaft engine/variable transmission combination. The sensitivity difference to design power needs a more detailed analysis to fully quantify any relative differences.

8. No first-order differences in sensitivity to fuel economy near the base values was calculated due to changes in single-shaft engine performance level.

APPENDIX A

Acronyms

AX	axial turbine stage
CAT	conventional automatic three-speed transmission
CVT	continuously variable speed-ratio transmission
FT	free turbine
RAD	radial turbine stage
SS	single shaft
VFTN	variable free-turbine nozzles
VIGV	variable compressor-inlet guide vanes
VOGV	variable compressor-outlet, or diffuser, guide vanes
VTN	variable turbine nozzles

APPENDIX B

Symbols

D	diameter, m; ft
E	heat exchanger heat-transfer effectiveness
g	acceleration due to gravity, 9.81 $(m/s^2)(Kg/N)$; 32.2 (ft/sec^2) (lbm/lbf)
J	mechanical equivalent of heat, 1 N-m/J; 778 ft-lbf/Btu
N	rotational speed, rpm
N_R	Reynolds number, $\frac{2w}{\mu D_m}$
N_{SC}	compressor specific speed, $\frac{\pi N \sqrt{Q_i}}{30\left[gJ(\Delta h')_{id}\right]^{3/4}}$
N_{ST}	turbine specific speed, $\frac{\pi N \sqrt{Q_o}}{30\left[gJ(\Delta h')_{id}\right]^{3/4}}$
p'	total pressure into component, N/cm^2; psi
p'_R	reference pressure, 10.132 N/cm^2; 14.696 psi
R	gas constant, J/kg-K; ft-lbf/^oR-lbm
R_R	reference gas constant, 287 J/kg-K; 53.3 ft-lbf/^oR-lbm
Q_i	impeller-inlet volume flow rate, m^3/s; ft^3/sec
Q_o	impeller-outlet volume flow rate, m^3/s; ft^3/sec
T'	total temperature into component, K; ^oR
T'_R	reference total temperature, 288.15 K; 518.67^oR
U	turbine-blade speed, m/s; ft/sec
w	mass-flow rate into component, kg/s; lbm/sec
W_{CE}	equivalent compressor mass-flow rate, $\frac{w\sqrt{\theta}}{\delta}$, kg/s; lbm/sec
W_{TE}	equivalent turbine mass-flow rate, $\frac{\varepsilon w\sqrt{\theta_{cr}}}{\delta}$, kg/s; lbm/sec

γ ratio of gas specific heats

γ_R reference ratio, 1.40

δ pressure ratio, p'/p'_R

Δh total-to-static enthalpy change, J/g; Btu/lbm

$\Delta h'$ total-to-total enthalpy change, J/g; Btu/lbm

$\Delta p'$ total-to-total pressure change, N/cm^2; psi

$\Delta\eta'_{vg}$ design-point total efficiency decrement due to presence of variable turbomachinery geometry

$\Delta\eta'_{pm}$ design-point total efficiency decrement due to difference between peak and design-point efficiency on component performance map

θ temperature ratio, T'/T'_R

θ_{cr} squared critical velocity ratio, $(T'/T'_R)\left(\frac{\gamma R}{\gamma + 1}\right)\Big/\left(\frac{\gamma_R R_R}{\gamma_R + 1}\right)$

ε specific heat function, $\frac{.7396}{\gamma}\left(\frac{\gamma + 1}{2}\right)^{\frac{\gamma}{\gamma-1}}$

λ turbine speed-work parameter, $U_m^2 \Big/ gJ(\Delta h')$

μ gas viscosity, kg/m-s; lbm/ft-sec

ν turbine blade-to-jet speed ratio, $U_t \Big/ \sqrt{2gJ(\Delta h)_{id}}$

τ torque, N-m; ft-lbf

Subscripts:

id ideal

m mean radius

opt optimum

t tip radius

Superscript:

* design

REFERENCES

1. Klann, J. L.; and Tew, R. C., Jr.: Analysis of Regenerated Single-Shaft Ceramic Gas-Turbine Engines and Resulting Fuel Economy In a Compact Car. NASA TM X-3531, 1977.

2. Klann, J. L.: Advanced Automotive Gas Turbine Analysis. Proceedings of Highway Vehicle Systems Contractors' Coordination Meeting, CONF-781050, U.S. Dept. of Energy, 1979, pp. 149-160.

3. Wagner, C. E.; and Pampreen, R. C.: Conceptual Design Study of Improved Automotive Gas Turbine Powertrain - Final Report. DOE/NASA/2749-79/3 Vol. 3, NASA CR-159672, 1980.

4. Johnson, R. A.: Conceptual Design Study of an Improved Gas Turbine (IGT) Powertrain. (DDA-EDR-9719, Detroit Diesel Allison; NASA Contract DEN3-28.) DOE/NASA/0028-79/1, NASA CR-159604, 1979.

5. Conceptual Design Study of Improved Automotive Gas Turbine Powertrain. (Ford Motor Company and AiResearch Manufacturing Company of Arizona; NASA Contract DEN3-37.) DOE/NASA/0037-79/1, NASA CR-159580, 1979.

6. Chapman, W. I.: Conceptual Design Study - Williams Research Corporation. Proceedings of the Sixteenth Highway Vehicle Systems Contractor's Coordination Meeting, CONF-7904105, U.S. Dept. of Energy, 1979, pp. 80-111.

7. Fishbach, L. H.; and Caddy, M. J.: NNEP - The Navy/NASA Engine Program. NACA TM X-71857, 1975.

8. Cook, J. A.; et al.: Ceramic Regenerator Systems Development Program. (Ford Motor Co.; NASA Contract DEN3-8.) DOE/CONS/0008-1, NASA CR-135330, 1977.

9. Wagner, C. E.; and Pampreen, R. C.: Upgraded Automotive Gas Turbine Engine Design and Development Program - Final Report. DOE/NASA/2749-79/2 Vol. 2, NASA CR-159671, 1980.

10. Galvas, M. R.: Fortran Program for Calculating Total-Efficiency - Specific-Speed Characteristics of Centrifugal Compressors. NASA TM X-2594, 1972.

11. McLallin, K. L.; and Kofskey, M. G.: Cold-Air Performance of Free Power Turbine Designed for 112-Kilowatt Automotive Gas-Turbine Engine. Vol. 2 - Effects of Variable Stator-Vane-Chord Setting Angle on Turbine Performance. DOE/NASA/1011-78/28, NASA TM-78993, 1979.

12. Galvas, M. R.: Fortran Program for Predicting Off-Design Performance of Centrifugal Compressors. NASA TN D-7487, 1973.

13. Glassman, A. J.: Computer Program for Preliminary Design Analysis of Axial-Flow Turbines. NASA TN D-6702, 1972.

14. Wasserbauer, C. A.; and Glassman, A. J.: Fortran Program for Predicting Off-Design Performance of Radial-Inflow Turbines. NASA TN D-8063, 1975.

15. Flagg, E. E.: Analytical Procedure and Computer Program for Determining the Off-Design Performance of Axial Flow Turbines. NASA CR-710, 1967.

16. Blumberg, P. N.: Powertrain Simulation: A Tool for the Design and Evaluation of Engine Control Strategies in Vehicles. SAE 760158, 1976.

Table I. Gas-turbine configurations.

No.	Shafting type	Turbine stages		Turbo-machinery geometry	Acronym[1]
		First	Second (or free)		
1	Single	Radial	-----	Fixed	SS/RAD
2				Variable	SS/RAD/VIGV
3				Variable	SS/RAD/VTN
4				Variable	SS/RAD/VOGV,VTN
5		Radial	Axial	Fixed	SS/RAD-AX
6		Axial	Axial	Fixed	SS/AX-AX
7	Free turbine	Radial	Axial	Fixed	FT/RAD-AX
8				Variable	FT/RAD-AX/VFTN
9		Axial	Axial	Fixed	FT/AX-AX
10				Variable	FT/AX-AX/VFTN

(1) Configuration acronyms are defined in Appendix A.

Table II. Gas-turbine engine and component parameter values assigned for configuration screening.

A. Gas-turbine engine parameters and values

Engine parameter	Value
Fuel	Gasoline
Lower heating value, J/g (Btu/lbm)	42500 (18300) (1)
Hydrogen-to-carbon mass ratio	.16
Ambient conditions (2)	
Temperature, ^{o}C (^{o}F)	29 (85)
Pressure, kN/m^2 (psia)	99.5 (14.431)
Net output power, kW (hp)	
Design	74.6 (100)
Idle	1.9 (2.5)

(1) English units were the base units in this study.

(2) SAE standard test conditions for gas-turbine engines.

Table II. Continued.

B. Gas-turbine component parameters and values.

Component	Parameter	Value
Inlet	Pressure drop ratio, $\Delta p'/p'$ [3]	
	Design	.015
	Off design	Fig. 1
Compressor	Efficiency, η'	
	Design base	Fig. 2
	Design decrements	
	Variable geometry, $\Delta\eta'_{vg}$	
	Inlet guide vanes (VIGV)	-.005
	Outlet guide vanes (VOGV)	-.020
	Performance maps, $\Delta\eta'_{pm}$	Table III
	Off design	fn (perf. maps)
	Outlet scroll pressure drop ratio, $\Delta p'/p'$	
	Design	.010
	Off design	Fig. 1
Regenerator	Heat transfer effectiveness	
	Design	.94
	Off design	Fig. 3
	Seal leakage mass flow rate	
	Design	Fig. 4
	Off design, %	Constant
	Distribution, %	
	Across cold face	30
	Carryover	30
	Across hot face	40
	Pressure drop ratio, $\Delta p'/p'$	
	Design	
	Cold side	.001
	Hot side	.029
	Off design	Fig. 1

[3] Symbols are defined in Appendix B.

Table IIB. Continued.

Component	Parameter	Value
Combustor	Efficiency	.99
	Pressure drop ratio, $\Delta p'/p'$	
	Design	.030
	Off design	Fig. 1
Turbine(s)	Inlet temperature, ^{o}C (^{o}F)	
	Design	1370 (2500)
	Off design[4]	$\leq$ 1370 ($\leq$ 2500)
	Design tip speed, m/s (ft/sec)	$\leq$610 ($\leq$ 2000)
	Efficiency, η'	
	Design base	Fig. 5 (radial) Fig. 6 (axial)
	Design decrements	
	Variable geometry, $\Delta\eta'_{vg}$	
	Radial nozzles (VTN)	-.01
	Axial nozzles (VFTN)	-.03
	Performance maps, $\Delta\eta'_{pm}$	Table III
	Off design	fn (perf. maps)
	Pressure drop ratio, $\Delta p'/p'$	
	Design	
	Inlet scroll	.010
	Interstage duct (FT only)	.025
	Outlet diffuser	.030
	Off design	Fig. 1
Exhaust	Design pressure drop ratio, $(\Delta p'/p')^{*}$	.020

[4] Varied such that turbine-outlet temperature was $\leq$ 1038^{o}C (1900^{o}F).

Table IIB. Concluded.

Component	Parameter	Value
Turbomachinery shaft(s)	Rotational speed (or defining parameters)	
	Single or gas generator, rpm	
	Design	100,000
	Idle	50,000
	Free turbine	
	Speed-work parameter, λ	1.0
	Hub-to-tip radius ratio	.7
	Stator exit angle	70^{o}
	Parastic load	
	Design, kW (hp)	
	Single or free-turbine	3 (4)
	Gas generator	.75 (1)
	Off design	Fig. 7
	Seal leakage mass-flow rate	
	Design	Fig. 4
	Off design, %	Constant
	Distribution, %	
	To turbine rotor inlet(s)[5]	100

[5] Configurations with two turbine stages were assumed to each receive half of the shaft-seal leakage flow.

Table III. Turbomachinery performance maps.

A. Map characteristics

Map type and number	Variable geometry	Source	Design pressure ratio	Design efficiency change, $\Delta\eta'_{pm}$
Compressor C1	----	Experiment[1]	4.08	-.03
C2	VIGV	Analytical	4.08	-.03
C3	VOGV	Experiment[2]	4.67	-.035
Radial Turbine RT1	----	Analytical	4.25	-.01
RT2	VTN	Analytical	4.25	-.04
RT3	----	Analytical	2.39	-.01
Axial turbine AT1	----	Analytical	2.10	-.015
AT2	----	Analytical	1.90	-.015
AT3	VFTN	Experiment[3]	1.70	0

[1] Ref. 9. [2] U.S. Army Taradcom [3] Ref. 11.

B. Configuration usage

Gas-turbine configuration		Compressor map number	Turbine map number	
No.	Acronym		First stage	Second stage
1	SS/RAD	C1	RT1	---
2	SS/RAD/VIGV	C2	RT1	---
3	SS/RAD/VTN	C1	RT2	---
4	SS/RAD/VOGV,VTN	C3	RT2	---
5	SS/RAD-AX	C1	RT3	AT1
6	SS/AX-AX	C1	AT2	AT1
7	FT/RAD-AX	C1	RT3	AT3
8	FT/RAD-AX/VFTN	C1	RT3	AT3
9	FT/AX-AX	C1	AT2	AT3
10	FT/AX-AX/VFTN	C1	AT2	AT3

Table IV. Total turbomachinery efficiency changes assigned at design point during screening.

Configuration		Total efficiency change ($\Delta\eta'_{vg} + \Delta\eta'_{pm}$)		
		Compressor	Turbines	
No.	Acronym		First	Second
1	SS/RAD	-.03	-.01	-----
2	SS/RAD/VIGV	-.035	-.01	-----
3	SS/RAD/VTN	-.03	-.05	-----
4	SS/RAD/VOGV,VTN	-.055	-.05	-----
5	SS/RAD-AX	-.03	-.01	-.015
6	SS/AX-AX	-.03	-.015	-.015
7	FT/RAD-AX	-.03	-.01	0
8	FT/RAD-AX/VFTN	-.03	-.01	-.03
9	FT/AX-AX	-.03	-.015	0
10	FT/AX-AX/VFTN	-.03	-.015	-.03

Table V. Car and fuel parameter values assigned for fuel economy analysis.

Parameter	Value
Fuel	Gasoline
Density, kg/ℓ (lbm/gal)	.743 (6.20)
Car	1978 compact
Test weight, kg (lbm)	1542 (3400)
Road-load power needs	Fig. 8
Accessory power needs	Fig. 9
Transmission	
Continuously variable speed ratio (CVT)	
Overall efficiency	Fig. 10
Conventional three-speed automatic (CAT)	
Transmission pump power needs	Fig. 9
Torque converter performance	Fig. 11
Gear box ratios	
First gear	2.45
Second gear	1.45
Third gear	1.00
Gear box efficiency	Fig. 12
Drive axle	
Gear ratio	2.53
Efficiency	.98
Wheels	
Rolling radius, m (ft)	.320 (1.05)
Moment of inertia (four wheels), $kg\text{-}m^2$ ($lbm\text{-}ft^2$)	4.51 (107)

Table VI. Differences in gas-turbine design values between base set and conservative set used for single-shaft sensitivity study.

Design parameter	Values	
	Conservative set	Base set
Regenerator effectiveness	.90	.94
Regenerator seal leakage[1]	Current	Advanced
Shaft speed, rpm	80,000	100,000
Shaft parasitic load, kW (hp)	6 (8)	3 (4)
Net idle-power output, kW (hp)	3.7 (5.0)	1.9 (2.5)
Additional efficiency decrements		
Compressor	-.02	0
Turbine	-.02	0
Combustor efficiency	.97[2]	.99

[1] See figure 4.

[2] Used only to simulate an engine heat loss.

Table VII. Comparison of measured and calculated fuel economies for the reference spark-ignition piston engine, three-speed automatic transmission, and vehicle.

Driving cycle	Fuel economies		
	Measured[1]	Calculated[2]	Calculated[3]
City, km/ℓ (mpg)	7.78 (18.3)	8.16 (19.2)	7.61 (17.9)
Highway, km/ℓ (mpg)	10.4 (24.5)	9.99 (23.5)	9.99 (23.5)
Composite, km/ℓ (mpg)	8.76 (20.6)	8.88 (20.9)*	8.54 (20.1)

[1]EPA data of February 1978.

[2]Without warm-up fuel.

[3]With warm-up fuel estimated.

*Reference fuel economy.

Table VIII. Comparison of results between models of a continuously variable transmission. Gas-turbine engine number 8, FT/RAD-AX/VFTN.

Driving cycle	Generalized model of fig. 10		Model of ref. 3	
	Fuel economy km/ℓ (mpg)	Average trans. efficiency	Fuel economy km/ℓ (mpg)	Average trans. efficiency
City	11.6 (27.3)	.74	11.3 (26.5)	.71
Highway	16.1 (37.8)	.76	16.4 (38.6)	.79
Composite	13.3 (31.2)	.75	13.1 (30.9)	.74

Table IX. Fuel economy screening results. All engines mated to generalized continuously variable speed-ratio transmission.

A. Comparisons among fixed-geometry engines.

Gas-turbine engine configuration, number - acronym	Best design pressure ratio	Composite fuel economy, km/ℓ (mpg)	Relative[1] fuel economy
1 - SS/RAD[2]	4.0	13.8 (32.4)	1.55
5 - SS/RAD-AX	4.5	13.6 (32.1)	1.54
6 - SS/AX-AX	4.5	13.5 (31.7)	1.52
7 - FT/RAD-AX	4.5	13.0 (30.5)	1.46
9 - FT/AX-AX	4.5	12.1 (28.4)	1.36

B. Comparisons among variable-geometry engines

Gas-turbine engine configuration, number-acronym	Best design pressure ratio	Composite fuel economy, km/ℓ (mpg)	Relative[1] fuel economy
4 - SS/RAD/VOGV,VTN[2]	3.5	14.9 (35.0)	1.67
3 - SS/RAD/VTN[2]	3.5	14.5 (34.2)	1.64
2 - SS/RAD/VIGV[2]	4.0	13.9 (32.8)	1.57
8 - FT/RAD-AX/VFTN	4.5	13.3 (31.2)	1.49
10 - FT/AX-AX/VFTN	4.5	13.0 (30.5)	1.46

[1] Relative to 8.88 km/ℓ (20.9 mpg) for spark-ignition engine in the same car.

[2] Turbine tip-speed limited to 610 m/s (2000 ft/sec).

Table X. Comparison of results between transmission types. Gas-turbine engine number 8, FT/RAD-AX/VFTN.

Driving Cycle	Fuel economy, km/ℓ (mpg)		Average transmission efficiency	
	CVT[1]	CAT[2]	CVT	CAT
City	11.6 (27.3)	12.2 (28.8)	.74	.76
Highway	16.1 (37.8)	17.7 (41.7)	.76	.85
Composite	13.3 (31.2)	14.2 (33.4)	.75	.80
Relative[3] composite	1.49	1.60		

[1] Generalized continuously variable speed-ratio transmission.

[2] Conventional automatic three-speed transmission.

[3] Relative to 8.88 km/ℓ (20.9 mpg) for spark-ignition engine in the same car.

Table XI. Sensitivity of composite fuel economy to small changes in gas-turbine design parameters.

Engine + transmission acronym	Percent change in fuel economy for a ±1% parameter change: 1-SS/RAD + CVT		8-FT/RAD-AX/ VFTN + CAT
Design engine values	Case A Base	Case B Cons.	Case C Base
Design parameter			
Regenerator effectiveness	±2.5	±2.5	±2.5
Turbine efficiency,			
Gas generator	±1.3	±1.3	± .8
Free turbine	NA(1)	NA	± .8
Combustor efficiency	+1.1	+1.1	±1.1
Compressor efficiency	± .8	± .8	± .8
Power output	∓ .4	∓ .4	∓ .1
Turbine-tip speed	± .3	± .4	NA
Gas-generator idle speed	-.2/+.3	-.2/+.3	∓ .4
Turbine-inlet temperature(2)			
With limited turbine-tip speed	(+.2/-.1)	(+.2/-.1)	NA
With optimum turbine-tip speed	(+.3/-.4)	(+.3/-.4)	(+.4/-.5)
Shaft speed			
Gas generator	NP(3)/-.1	± .1	NP/-.1
Free turbine	NA	NA	NP/-.07
All component pressure drops	∓ .1	∓ .1	∓ .1
Shaft parasitic load	∓ .07	∓ .1	∓ .08
Regenerator leakage flow rate	∓ .05	∓ .1	∓ .05
Idle power output	∓ .03	∓ .07	∓ .03

(1) NA - Not applicable.

(2) No turbine-outlet temperature limit.

(3) NP - Not possible.

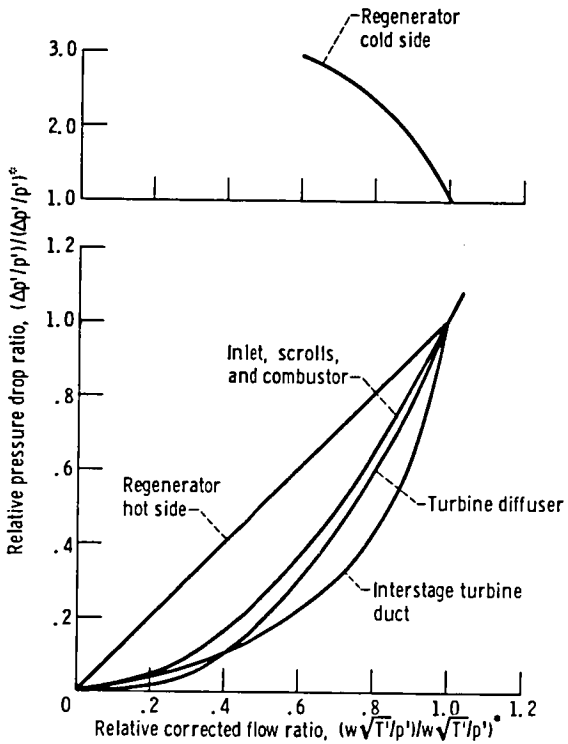

Figure 1. - Component pressure drop variations.

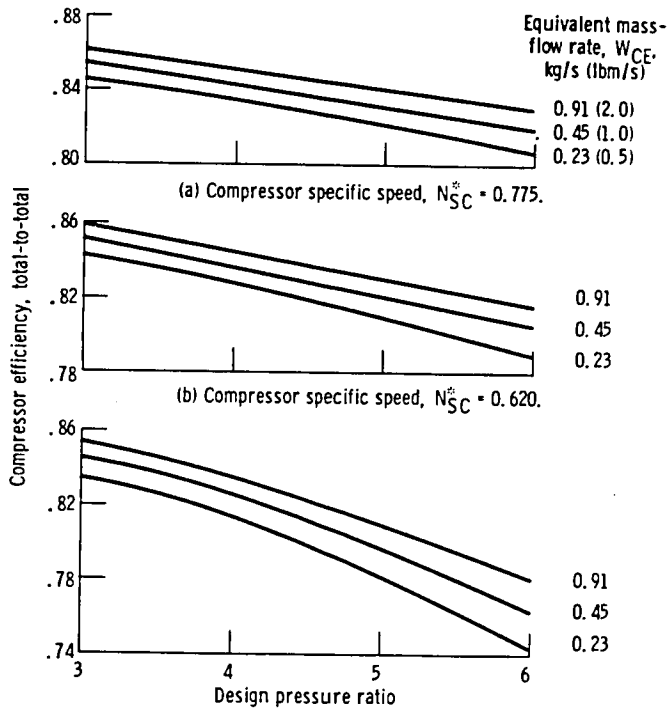

(c) Compressor specific speed, N^*_{SC} = 0.465.

Figure 2. - Basic correlations for peak compressor efficiency.

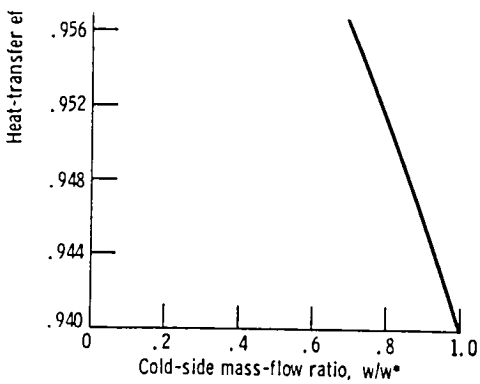

Figure 3. - Regenerator effectiveness variation.

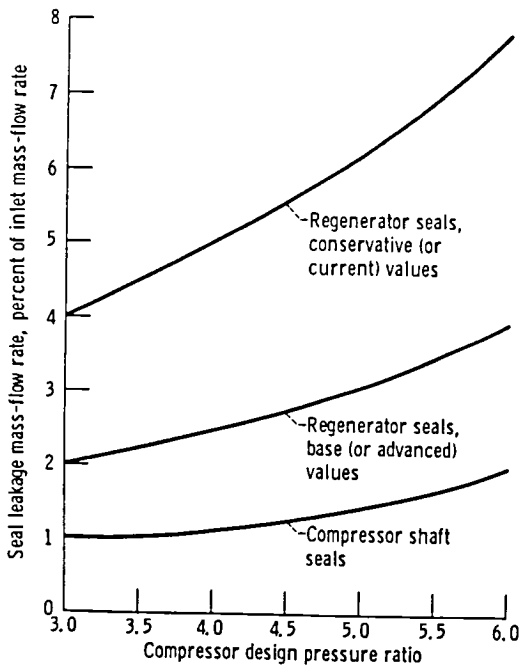

Figure 4. - Seal leakage flow rates.

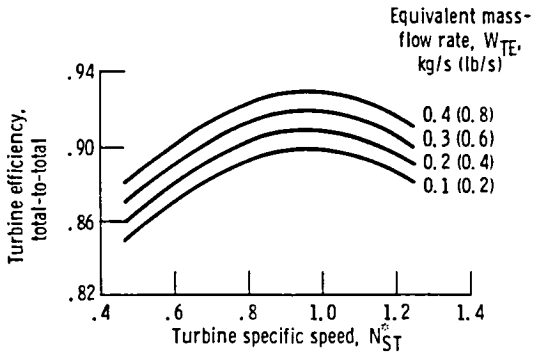

(a) Efficiencies for optimum blade-to-jet speed ratio, ν^*_{opt}.

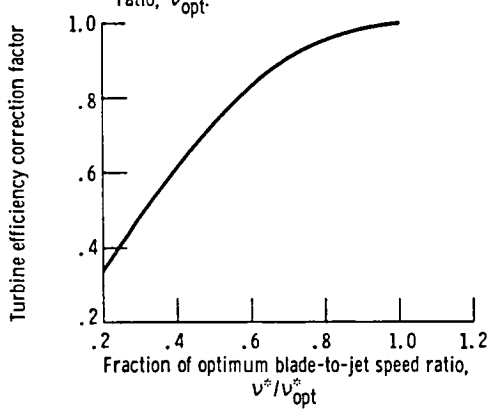

(b) Tip-speed correction.

Figure 5. - Basic correlations for peak radial-flow turbine efficiency.

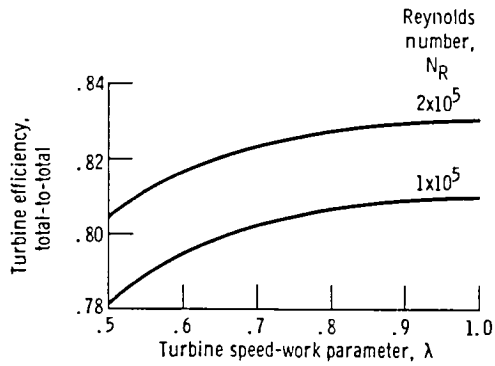

Figure 6. - Basic correlations for peak axial-flow turbine efficiency.

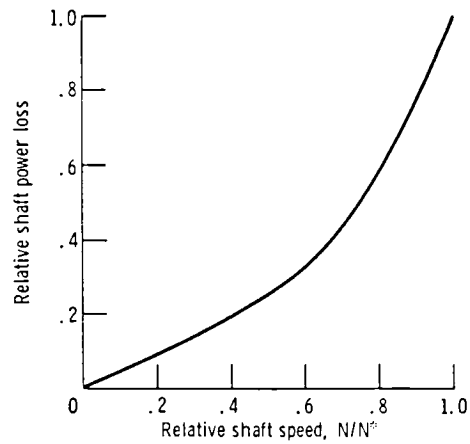

Figure 7. - Shaft parasitic power loss variation.

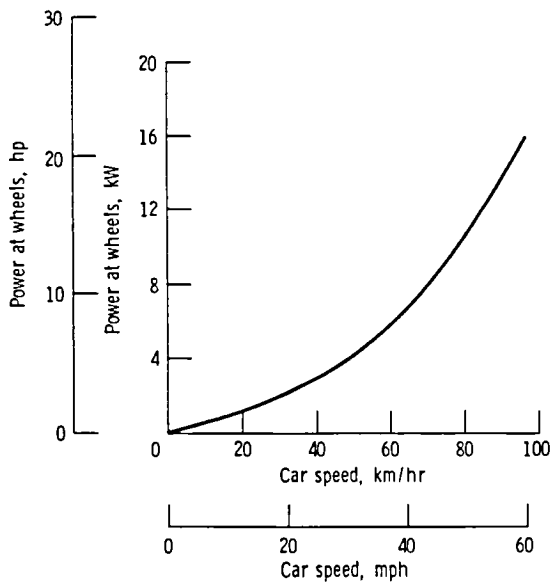

Figure 8. - Car road-load power needs.

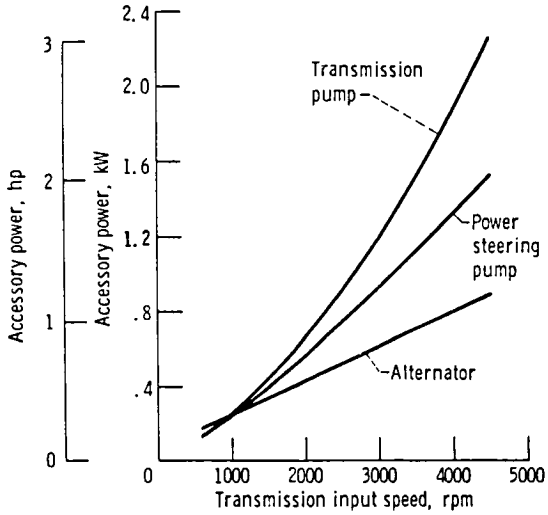

Figure 9. - Car accessory and transmission pump power needs.

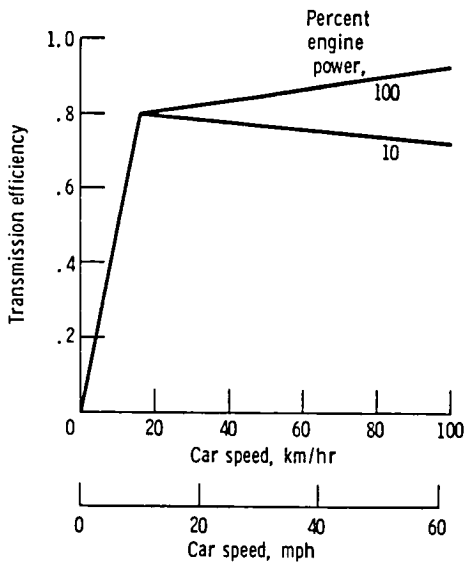

Figure 10. - Generalization for overall efficiency of a continuously variable speed-ratio transmission.

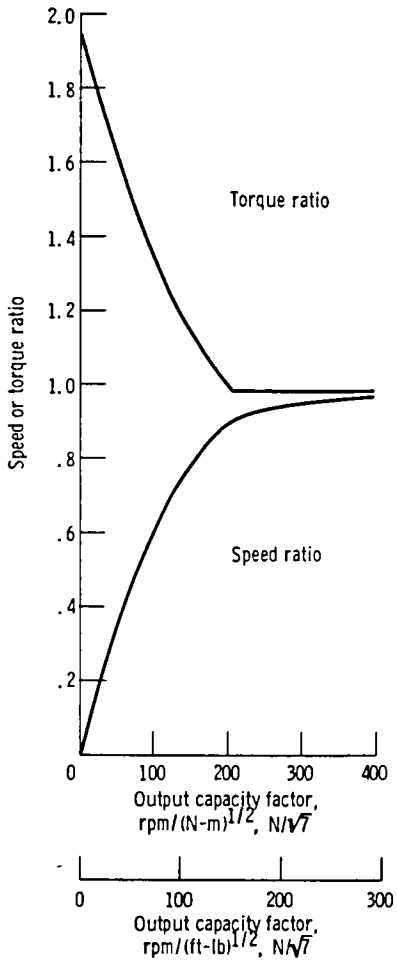

Figure 11. - Torque converter performance.

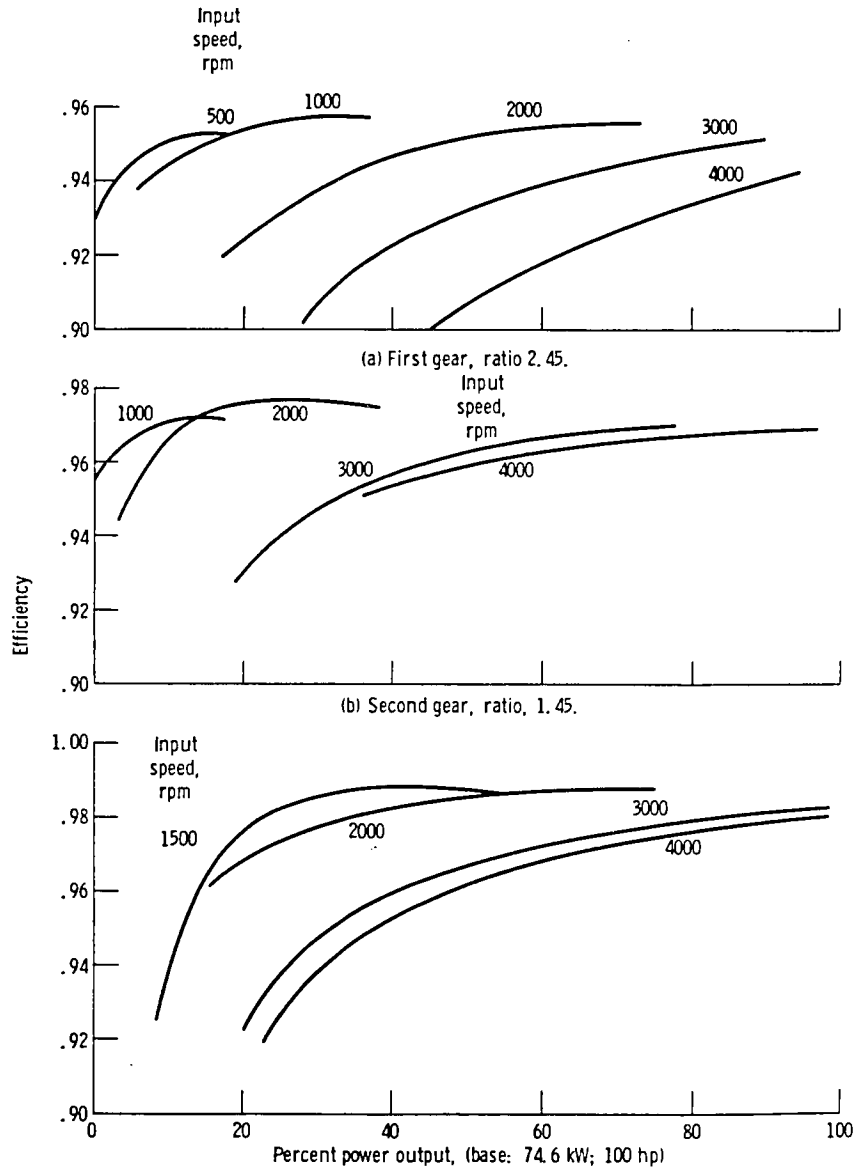

Figure 12. - Transmission gear-box efficiencies.

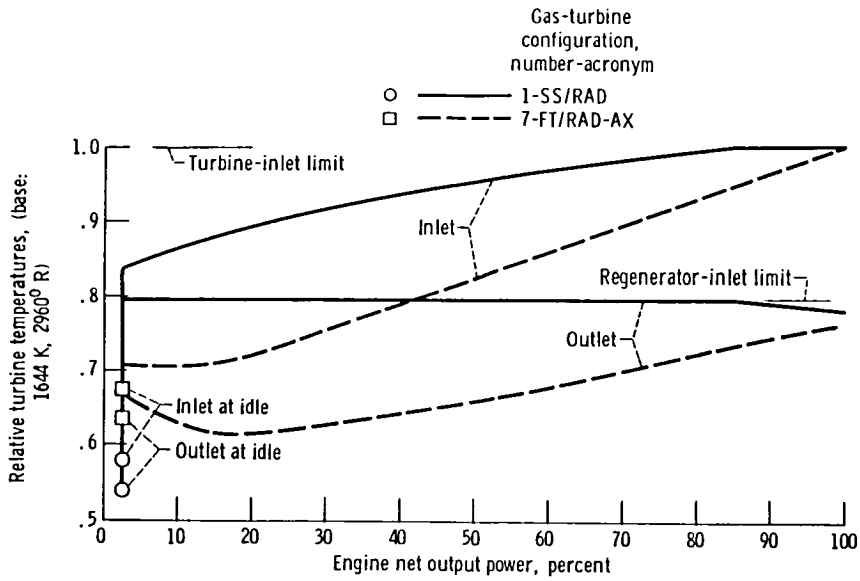

Figure 13. - Turbine operating temperature comparisons between engines.

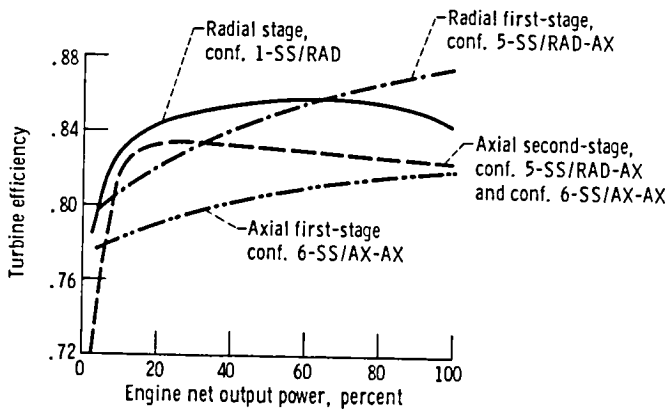

Figure 14. - Turbine-stage efficiency comparisons among fixed-geometry single-shaft engines.

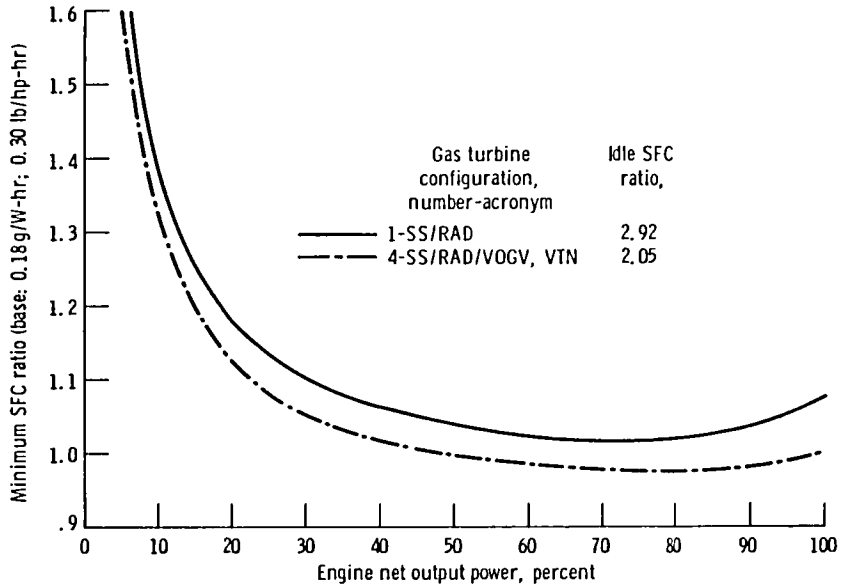

Figure 15. - Effect of variable turbomachinery geometry on engine performance.

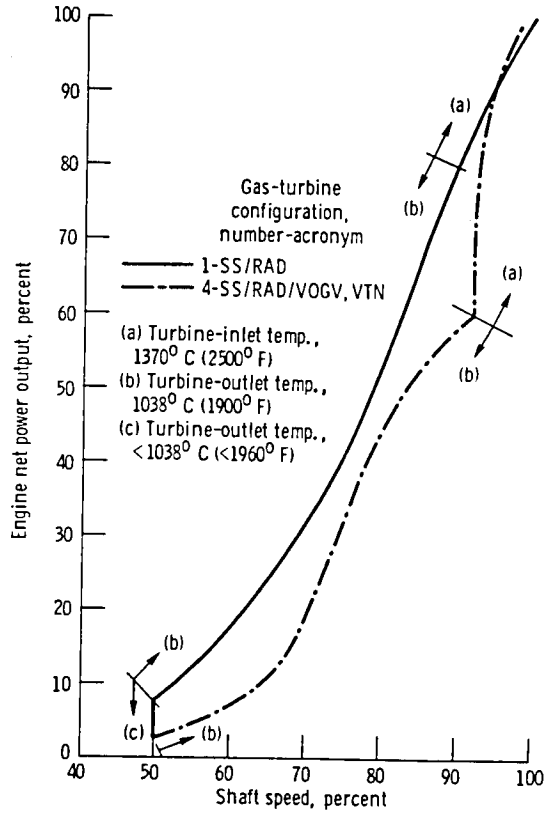

Figure 16. - Effect of variable geometry on engine speed-power relationship.

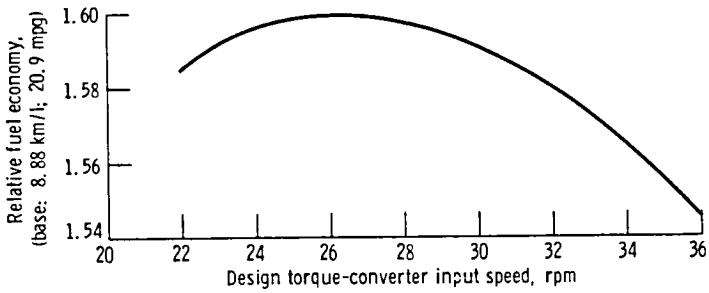

Figure 17. - Effect of rated torque converter speed on composite fuel economy. Configuration: 8-FT/RAD-AX/VFTN + CAT.

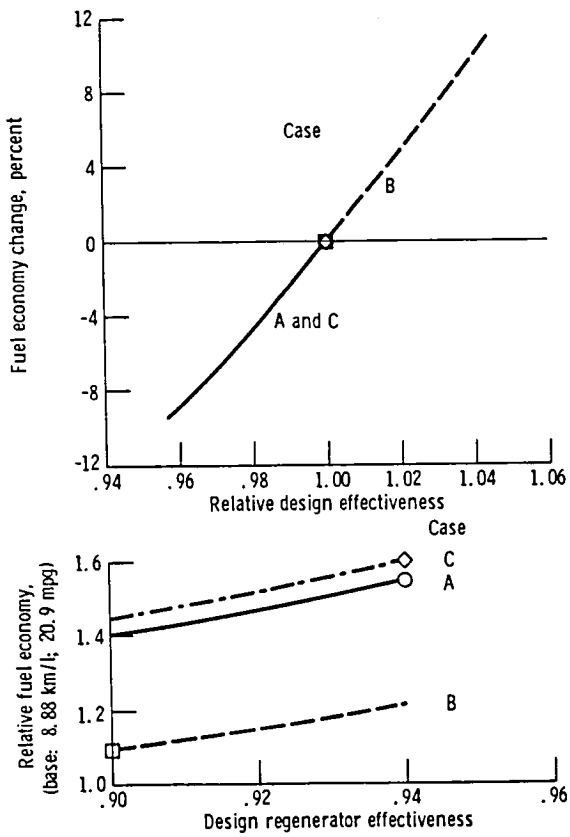

Figure 18. - Effect of design regenerator effectiveness on composite fuel economy. Symbols show base values. See table XI for cases.

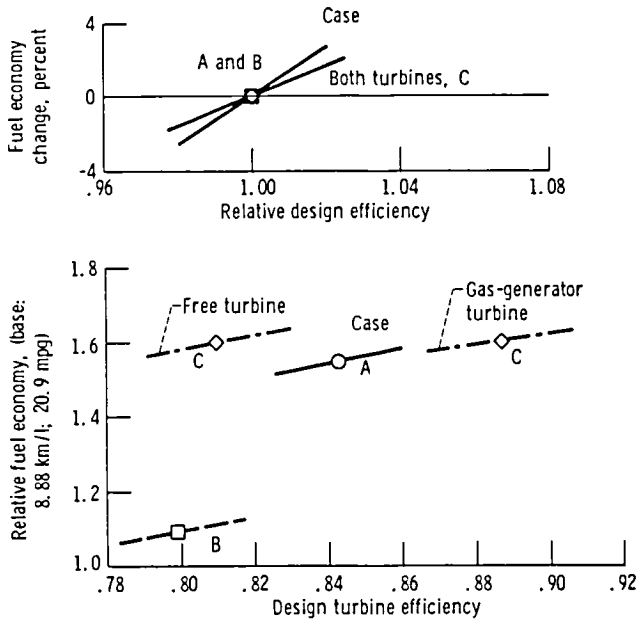

Figure 19. - Effect of design turbine efficiency on composite fuel economy. Symbols show base values. See table XI for cases.

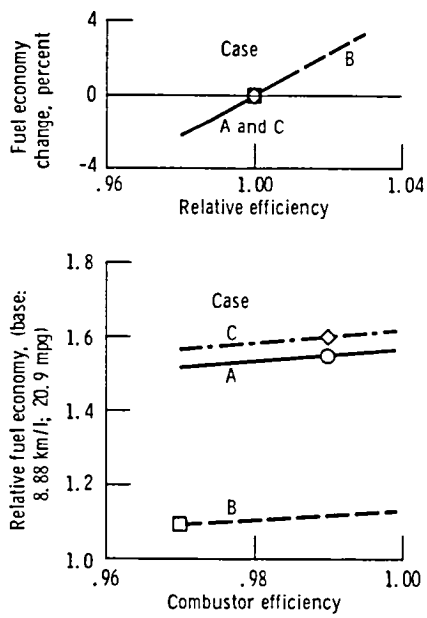

Figure 20. - Effect of combustor efficiency on composite fuel economy. Symbols show base values. See table XI for cases.

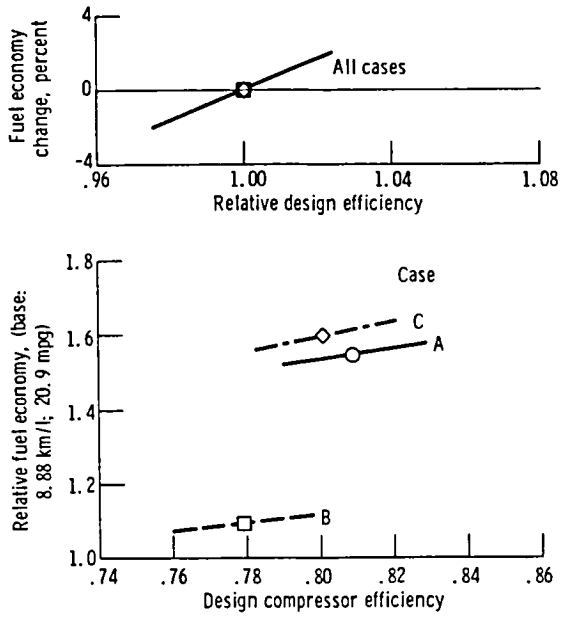

Figure 21. - Effect of design compressor efficiency on composite fuel economy. Symbols show base values. See table XI for cases.

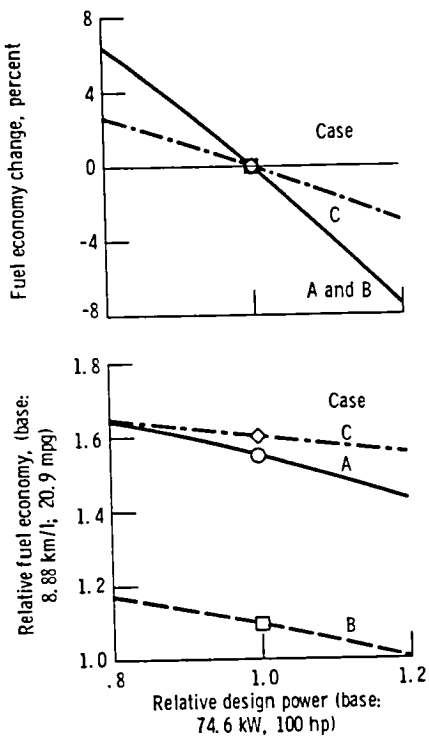

Figure 22. - Effect of design net power output on composite fuel economy. Symbols show base values. See table XI for cases.

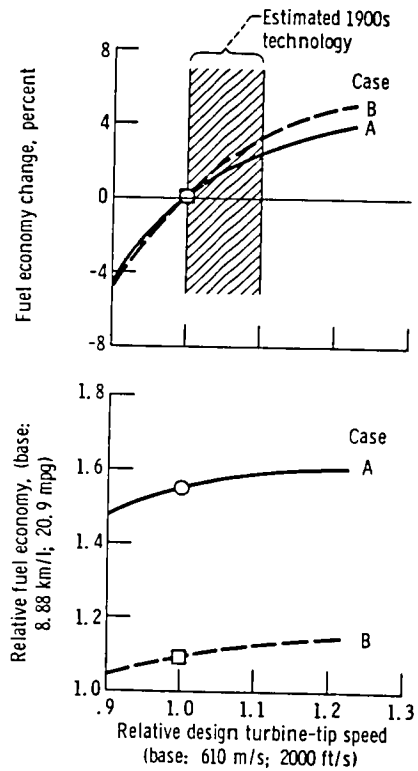

Figure 23. - Effect of design radial turbine-tip speed on composite fuel economy. Symbols show base values. See table XI for cases.

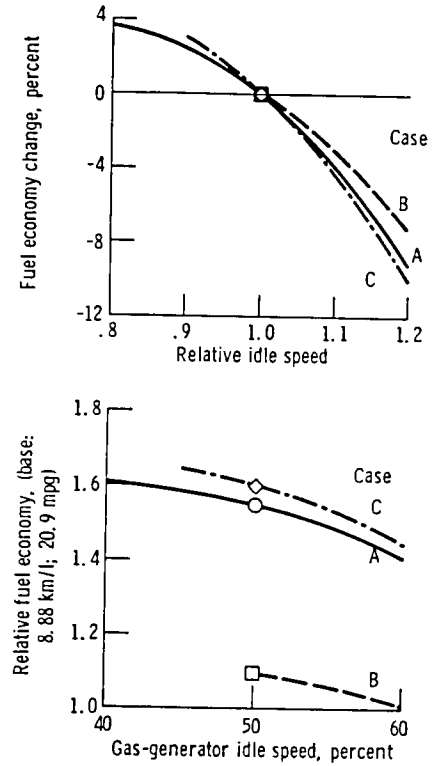

Figure 24. - Effect of idle speed on composite fuel economy. Symbols show base values. See table XI for cases.

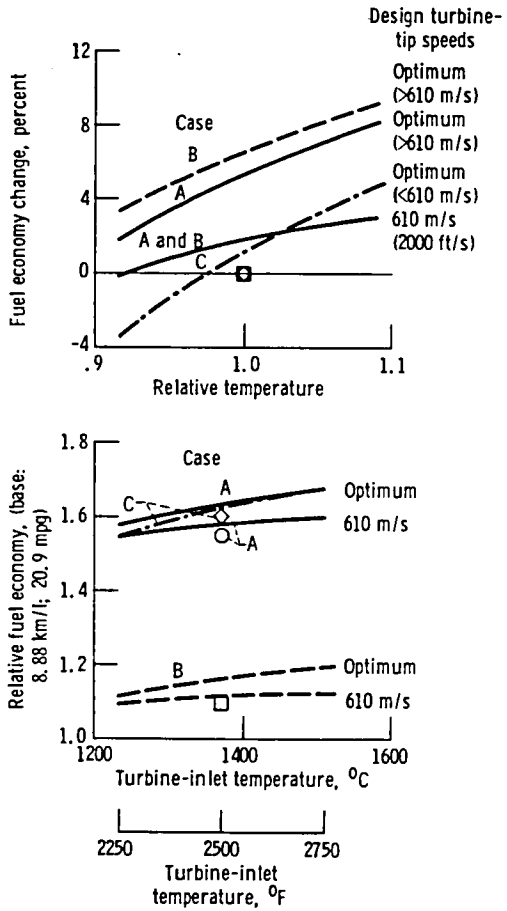

Figure 25. - Effect of turbine-inlet temperature on composite fuel economy. No regenerator-temperature limit. Symbols show base values. See table XI for cases.

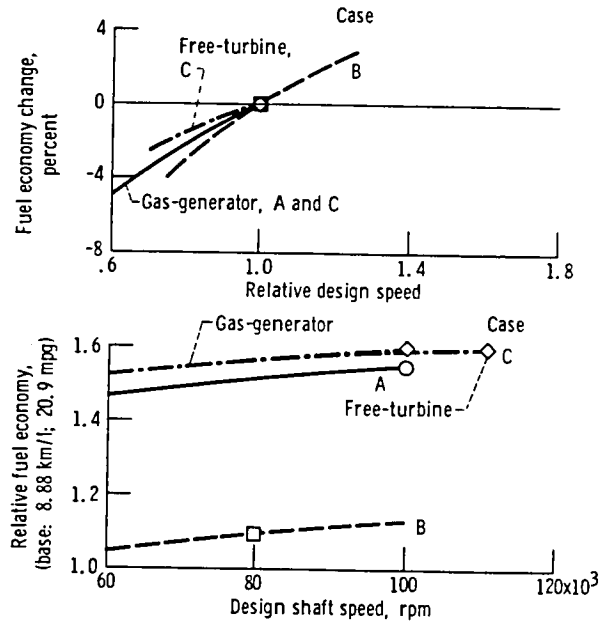

Figure 26. - Effect of design shaft speed on composite fuel economy. Symbols show base values. See table XI for cases.

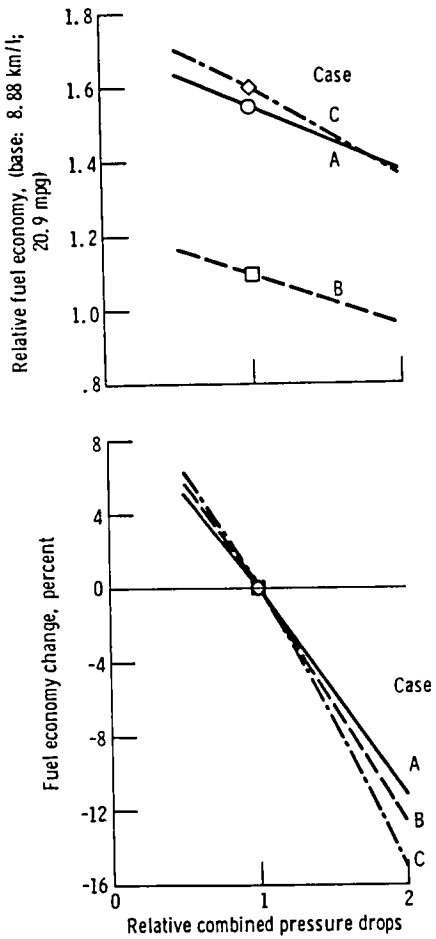

Figure 27. - Effect of combined changes in design pressure drops on composite fuel economy. Symbols show base values. See table XI for cases. See table II for base pressure drop ratios.

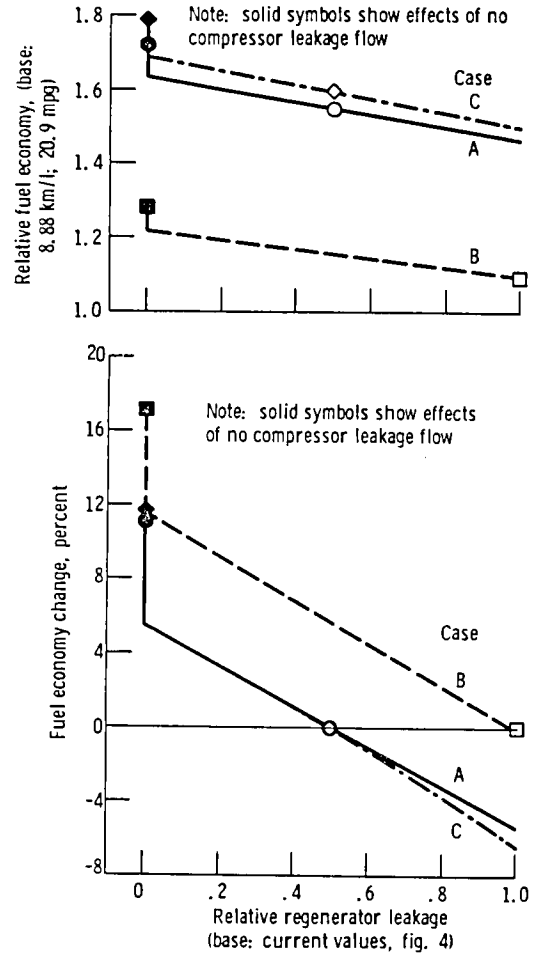

Figure 28. - Effects of relative seal-leakage mass-flow rates on composite fuel economy. Open symbols show base values. See table XI for cases.

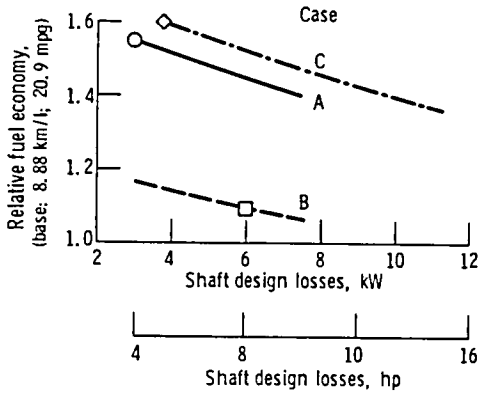

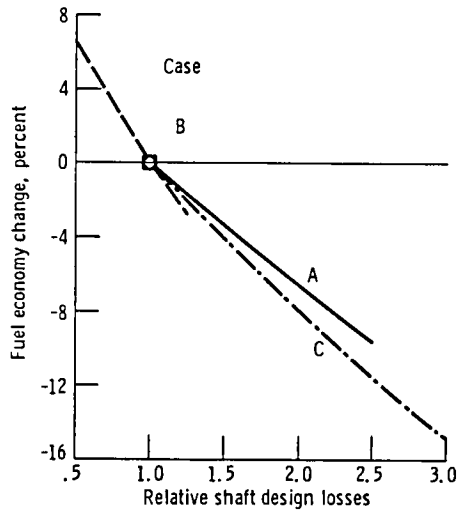

Figure 29. - Effect of design engine-shaft losses on composite fuel economy. Symbols show base values. See table XI for cases.

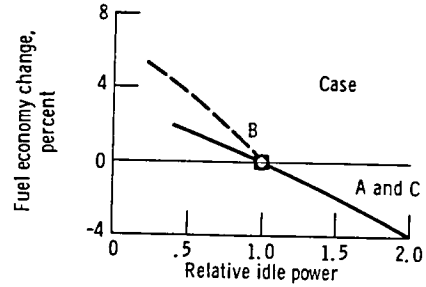

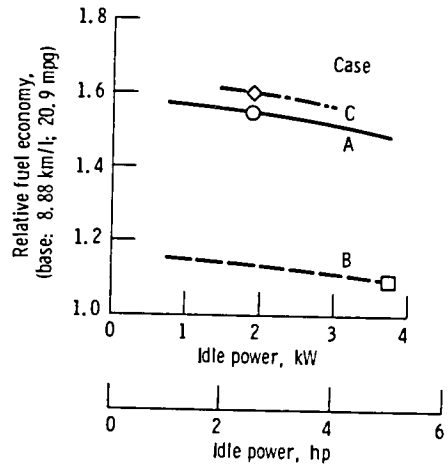

Figure 30. - Effect of idle power on composite fuel economy. Symbols show base values. See table XI for cases.

1. Report No.	2. Government Accession No.	3. Recipient's Catalog No.
NASA TM-81433		

4. Title and Subtitle	5. Report Date
FUEL ECONOMY SCREENING STUDY OF ADVANCED AUTOMOTIVE GAS TURBINE ENGINES	March 1980
	6. Performing Organization Code

7. Author(s)	8. Performing Organization Report No.
John L. Klann	E-357
	10. Work Unit No.

9. Performing Organization Name and Address	11. Contract or Grant No.
National Aeronautics and Space Administration Lewis Research Center Cleveland, Ohio 44135	

12. Sponsoring Agency Name and Address	13. Type of Report and Period Covered
U.S. Department of Energy Transportation Energy Conservation Division Washington, D.C. 20545	Technical Memorandum
	14. Sponsoring Agency Code Report No. DOE/NASA/1040-80/11

15. Supplementary Notes

Final report. Prepared under Interagency Agreement EC-77-A-31-1040.

16. Abstract

Fuel economy potentials were calculated and compared among 10 turbomachinery configurations. All gas-turbine engines were evaluated with a continuously variable transmission in a 1978 compact car. A reference fuel economy was calculated for the car with its conventional spark-ignition piston engine and three-speed automatic transmission. The best free-turbine engine was also evaluated with the conventional transmission. Two promising engine/transmission combinations, using gasoline, had 55 to 60 percent gains over the reference fuel economy. Fuel economy sensitivities to engine design parameter changes were also calculated for these two combinations.

17. Key Words (Suggested by Author(s))	18. Distribution Statement
Automotive gas turbines Fuel economy analysis Advanced engines Ceramic turbines	Unclassified - unlimited STAR Category 85 DOE Category UC-96

19. Security Classif. (of this report)	20. Security Classif. (of this page)	21. No. of Pages	22. Price*
Unclassified	Unclassified		

* For sale by the National Technical Information Service, Springfield, Virginia 22161